Identification of Umbre Orthobunyavirus as a Novel Zoonotic Virus Responsible for Lethal Encephalitis in 2 French Patients With Hypogammaglobulinemia

Philippe Perot, Franck Bielle, Thomas Bigot, Vincent Foulongne, Karine Bolloré, Delphine Chrétien, Patricia Gil, Serafin Gutierrez, Grégory L'ambert, Karima Mokhtari, et al.

Title

Identification of Umbre Orthobunyavirus as a Novel Zoonotic Virus Responsible for Lethal Encephalitis in Two French Patients with Hypogammaglobulinemia

Authors

Philippe Pérot[1], Franck Bielle[2,3], Thomas Bigot[4], Vincent Foulongne[5], Karine Bolloré[5], Delphine Chrétien[1], Patricia Gil[6,7], Serafín Gutiérrez[6,7], Grégory L'Ambert[8], Karima Mokhtari[2,3], Jan Hellert[9], Marie Flamand[9], Carole Tamietti[9], Muriel Coulpier[10], Anne Huard de Verneuil[10], Sarah Temmam[1], Thérèse Couderc[11], Edouard De Sousa Cunha[2], Susana Boluda[2,3,19], Isabelle Plu[2,3,19], Marie Bernadette Delisle[12], Fabrice Bonneville[13], David Brassat[14], Claire Fieschi[15], Marion Malphettes[15], Charles Duyckaerts[2,3], Bertrand Mathon[3,16], Sophie Demeret[17], Danielle Seilhean[2,3,19**], Marc Eloit[1,18*]

[1] Pathogen Discovery Laboratory, Institut Pasteur, Paris (75015), France

[2] Département de Neuropathologie Raymond Escourolle, AP-HP-Sorbonne, Groupe Hospitalier Pitié-Salpêtrière, Paris, France

[3] Sorbonne Université, Brain Institute (ICM; INSERM, UMRS 1127; CNRS, UMR 7225), Paris, France

[4] Hub de Bioinformatique et Biostatistique – Département Biologie Computationnelle, Institut Pasteur, USR 3756 CNRS, Paris, France

[5] Pathogenesis and Control of Chronic Infections. INSERM, University of Montpellier, Etablissement Français du Sang, CHU Montpellier, Montpellier, France

[6] CIRAD, UMR ASTRE, F-34398 Montpellier, France

[7] ASTRE, CIRAD, INRA, University of Montpellier, Montpellier, France

[8] EID Méditerranée, Montpellier, France

[9] Structural Virology Unit, Institut Pasteur, CNRS UMR 3569, Paris (75015), France

[10] UMR Virologie, ANSES, ENVA, INRAE, UPE, Ecole Nationale Vétérinaire d'Alfort, 7 Av du Gal de Gaulle, F-94704, Maisons-Alfort, France

[11] Biology of Infection Unit, Institut Pasteur, Inserm U1117, Paris (75015), France

[12] Laboratoire de Neuropathologie, Laboratoire universitaire d'anatomie et cytologie pathologiques, CHU de Toulouse, Université Toulouse III - Paul Sabatier, Toulouse, France

[13] Department of Neuroradiology, CHU de Toulouse and UMR 1214 ToNIC, Université de Toulouse, Inserm, France

[14] CRC-SEP, Pole des Neurosciences CHU Toulouse and UMR 1043, Université de Toulouse III, Toulouse, France

[15] Service d'immunologie clinique, Hôpital Saint-Louis, Assistance Publique-Hôpitaux de Paris, Université de Paris, France

[16] AP-HP, Hôpitaux Universitaires Pitié-Salpêtrière Charles-Foix, Department of Neurosurgery, Paris, France

[17] Department of Neurology, Neuro ICU, Groupe Hospitalier Pitié-Salpêtrière, AP-HP, Paris, France.

[18] Ecole Nationale Vétérinaire d'Alfort, Maisons-Alfort, France

[19] CNR ATNC (Reference Center for Non-Conventional Transmissible Agents), Laboratory and neuropathology network for the surveillance of Creutzfeldt-Jakob Disease, Santé Publique France, AP-HP, Paris, France.

[*] Corresponding author: Marc Eloit marc.eloit@pasteur.fr +33(0)144389216

[**] Alternate corresponding author: Danielle Seilhean danielle.seilhean@aphp.fr +33(0)142161891

Keywords

Encephalitis; Umbre Virus; Orthobunyavirus; Metatranscriptomics; Next Generation Sequencing

Running title

Umbre Virus Encephalitis

Summary of the article's main point (40-word summary)

- First cases of Umbre orthobunyavirus human infection.
- Lethality in immunocompromised patients.
- Arguments for transmission by *Culex pipiens* mosquitoes in France.
- No specific immune response detected in control populations.

Abstract

Background

Human encephalitis represents a medical challenge from a diagnostic and therapeutic point of view. We investigated the cause of two fatal cases of encephalitis of unknown origin in immunocompromised patients.

Methods

Untargeted metatranscriptomics was applied on two patient's brain tissue to search for pathogens (viruses, bacteria, fungi, or protozoans) without prior hypothesis.

Results

Umbre arbovirus, an orthobunyavirus never identified in humans until now, was found in two patients. *In situ* hybridization and RT-qPCR showed that Umbre virus infected neurons and replicated at high titers. The virus was not detected in CSF by RT-PCR. Viral sequences related to Koongol virus, another orthobunyavirus close to Umbre virus, were found in *Culex pipiens* mosquitoes captured in the south of France where the patients had spent some time before the onset of symptoms, demonstrating the presence of the same clade of arboviruses in Europe and its potential public health impact. A serological survey conducted in the same area did not identify positive individuals for Umbre virus. The absence of seropositivity in the population may not reflect the actual risk of disease transmission in immunocompromised individuals.

Conclusions

Umbre arbovirus can cause encephalitis in immunocompromised humans and is present in Europe.

Introduction

Human encephalitis is a potentially fatal disease of the central nervous system that is frequently associated with neurological sequelae. The incidence is about 1.5 - 7 cases / year / 100,000 inhabitants. In 20-50% of cases, encephalitis with known etiology is related to infection [1], most often of viral origin. The most frequently implicated viruses belong to the *Herpesviridae* family (Herpes Simplex virus, Varicella Zoster virus, etc.), but also, depending on the geographical area, to arboviruses such as Japanese encephalitis virus (JEV, in Asia) and tick-borne encephalitis virus (TBEV, in Europe and Northeast Asia). In more than a third of the cases, the etiology of encephalitis is, however, unknown, even in countries benefiting from high-performance diagnostic technologies [2]. Indeed, new pathogens responsible for encephalitis are regularly identified [3]. Diagnosis of encephalitis is also challenging because of the geographical spread of neurotropic arboviruses favored by climate change and human migration. In addition, this spread exposes human or animal populations devoid of specific immunity to these newly introduced arboviruses [4]. A recent example is the Usutu virus, a flavivirus of the JEV complex responsible for human encephalitis, which has recently expanded in Europe [5]. Here, using agnostic metatranscriptomics procedures, we analyzed the brain tissue from two fatal cases of encephalitis for which a viral etiology had been suspected, and found evidence of infection by Umbre virus, a mosquito orthobunyavirus never described in humans before.

Case reports

Case 1

A 21-year-old man was admitted to the neurology department of Toulouse Hospital in October 2013 for swallowing impairment and fluctuation of consciousness. He was living in Moissac, in the south-west of France. He had developed behavioral changes suggestive of depression after a party during which he could have used cocaine and cannabis. His psychiatrist had prescribed selective serotonin reuptake inhibitors. The clinical state had not improved. He was then referred to the psychiatry department at Toulouse University Hospital. He had a medical history of Bruton agammaglobulinemia (Omim **#** 300755), an X-linked immunodeficiency characterized by the absence of circulating B cells and low to undetectable levels of all immunoglobulin isotypes in the serum. He was treated since childhood by intravenous immunoglobulins together with an anti-infectious prophylaxis by valaciclovir and sulfamethoxazole/trimethoprim. He was also suffering from Crohn disease treated with mesalazine and azathioprine.

The patient was anorectic and had lost 10 kg during the last weeks. He was afebrile. The diagnosis of catatonia was considered. He did not respond to antidepressants, benzodiazepines and neuroleptics at high doses. Upon admission in the Neurology department, brain MRI, with FLAIR (FLuid-Attenuated Inversion Recovery) sequence and diffusion-weighted imaging, showed a diffuse hypersignal in the insular, posterior cingulate and occipital cortices, and in the caudate nucleus and putamen, bilaterally (**Figure 1, a & b**). FDG PET/CT scan showed a diffuse cortical hypofixation, more severe in the left hemisphere and no hypermetabolism outside the brain. Blood cell count showed a decreased number of lymphocytes (500 G/L). There was no anti-thyroglobulin and anti-thyroperoxidase antibody in the serum. Serological tests for *Borrelia burgdorferi*, *Treponema pallidum*, polyomavirus, HIV, and hepatitis B, C, and E viruses were negative – a negativity that was difficult to interpret in a patient with agammaglobulinemia. The concentration of serum C-reactive protein was increased (150 mg/L; normal

value below 6 mg/L). The blood levels of aspartate aminotransferase, and alanine aminotransferase were increased two folds.

Total proteins concentration, glucose level, and cell count were normal in the cerebrospinal fluid (CSF). No oligoclonal bands were detected. CSF PCRs for enteroviruses, herpesviruses, and *Tropheryma whipplei* were negative. The search for Ri/La/Hu, VGCC, NMDA receptor, GABA, ANNA-1, ANNA-2, gangliosides, AQP4, and MOG antibodies was negative. The CSF was positive for the 14-3-3 protein.

The patient died two months and a half after the first symptoms. The rapid course of the disease, the cortical and striatal hyperintensity at MRI, the positivity of 14-3-3 protein in the CSF, and a history of repeated treatment with blood products had raised the diagnostic hypothesis of Creutzfeldt-Jakob disease, either iatrogenic or variant. The diagnosis of encephalitis, by contrast, was thought implausible: the patient had been afebrile during the whole course of the disease and the CSF cell count was normal. The autopsy was limited to the brain. The brain samples were referred to the national neuropathology network for the surveillance of Creutzfeldt-Jakob disease.

Case 2

A 58-year-old woman was referred to the emergency department of Paris Pitié-Salpêtrière Hospital in October 2018 for anorexia and psychomotor slowing, without fever. She had been followed in the immunology department (Saint Louis Hospital, Paris) for a complex immunologic disorder. The diagnosis of a cutaneous follicular lymphoma had been made 17 years earlier. She had been treated with radiotherapy, surgery and chemotherapy (rituximab-cyclophosphamide-vincristin-prednisone, then rituximab-cyclophosphamide). She had been in complete remission for 9 years. She had developed a humoral immune deficiency characterized by low IgG and undetectable IgM levels in the absence of circulating B cells. She had recurrent bacterial infections for which she had received polyvalent immunoglobulins. She was also suffering from vitiligo and lichen planus. She had been followed for more than 10 years for a severe autoimmune hepatitis requiring immunosuppressive treatment with sirolimus and leading to cirrhosis, for which transplantation was being considered.

At admission in the intensive care unit, psychomotor slowing was marked. There were no focal neurological signs. CSF was clear and contained 10 white blood cells/mm^3 (N<5), with CD20 negative lymphocytes at various stages of activation and some macrophages. CSF glucose was normal (3.53 mmole/L). The protein level was increased (0.67 g/L, N< 0.40). MRI was normal (**Figure 1, c-e**). Three months later, the patient was apathetic. The CSF contained 34 white blood cells/mm3 and 4,200 red blood cells/mm3. CSF protein level was 0.47 g/L. Interferon alpha was increased in the CSF (6 kUI/L, N<2), normal in the serum (2 kUI/L). The search for autoantibodies (including NMDAr, Yo, RI, Hu, amphiphysine, CV2, Sox1, GAD, Ma1, Ma2) was negative. CSF PCRs for viruses (EBV, CMV, HSV1 and 2, VZV, HHV6, HHV8, adenovirus, enterovirus, polyomavirus) were all negative. She received intravenous immunoglobulins in the hypothesis of dysimmune encephalitis. Four months later, her neurologic condition worsened. She had lost her balance, had fallen several times and was mute. She was transferred to the neurology department at Pitié-Salpêtrière Hospital. She lived in Paris area (Val-de-Marne). Her relatives indicated that she had traveled extensively, visiting China, Japan, Australia, Spain, Israel and Italy in previous years. They also reported that a few weeks before the onset of the symptoms, she had sojourned in Camargue, south of France, and went on a 10-day Mediterranean cruise.

Despite treatment with amoxicillin and aciclovir, she progressed to akinetic mutism within three months. Hyperintensity in the hippocampus, the temporal pole and the insula were observed bilaterally and progressed to atrophy (**Figure 1, f-h**). The spinal MRI was normal. Repeated EEG showed slow waves, with pseudo-periodic patterns, similar to those observed in Creutzfeldt-Jakob disease. She became comatose, despite Ig replacement therapy, high dose steroids pulses, and plasma exchange in the hypothesis of autoimmune encephalitis. It was decided to perform a biopsy of the right frontal middle gyrus in the absence of focal lesion visible at MRI.

Nine days after the biopsy, the patient developed acute hepatic failure due to portal venous thrombosis. She died after an evolution of five months and a half. The diagnosis of encephalitis was suspected but its cause remained undetermined. An autopsy was performed.

Methods

Methods are described in the **Supplementary Material (online resource)**.

Results

Neuropathology

Case 1

The brain weighed 1200 g. Its external aspect was unremarkable. Microscopic examination showed severe neuronal loss and spongiosis in the cerebral cortex and in the striatum in both hemispheres (**Supplementary Table 1; Figure 2, d**); the number of Purkinje cells was also severely reduced. The gliosis was marked, made of fibrillar astrocytes with abundant eosinophilic cytoplasm**.** Microglia -IBA1, CD163 and CD68 positive- were diffusely activated (**Figure 2, a-c; Supplementary Table 2**). Numerous microglial nodules were observed, in particular in the pyramidal layer of the hippocampus and in the dentate nucleus of the cerebellum (**Figure 2, a & b**). The nodules sometimes contained a neuron (neuronophagia) (**Figure 2, a**). A few T lymphocytes, CD3 and CD8 positive, were diffusely distributed around the vessels and in the parenchyma (**Figure 2, e**). CD20 and CD4 immunohistochemistry was negative (**Figure 2, d & e**). No viral inclusion was observed. Luxol Fast Blue staining did not show significant demyelination. PrP 12F10 immunohistochemistry was negative as well as the PrPres Western blot.

Case 2 biopsy

The biopsy sample consisted of 1 cm^3 of cerebral cortex comprising leptomeninges, gray and white matter. Microscopic examination showed marked astrogliosis and severe microglial activation, confirmed by CD163 immunochemistry. Some perivascular cuffs were observed, made of CD3 positive, small T-lymphocytes, 80% of them being CD4- and 20%, CD8-positive. There was no granuloma nor multinucleated giant cell.

Case 2 autopsy

The brain weighed 1055 g. Gross examination showed thinning and softening of the temporal poles, and atrophy of the caudate nucleus and cerebral peduncles, bilaterally. An inflammatory infiltrate of low abundance, made of small CD3 positive T lymphocytes, was observed in the leptomeninges and around the veins in the caudate nucleus and mesencephalon (**Supplementary Table 1**). The arterial walls were not altered; there was no evidence for vasculitis. Severe neuronal loss, astrogliosis, and diffuse microglial activation were observed in the neocortex, hippocampus, striatum and cerebellum on both sides (**Supplementary Table 1; Figure 3, a & b**). There was a severe loss of pyramidal neurons in CA1 to CA4 sectors (**Figure 3, d**). Neurons were replaced by reactive astrocytes with enlarged cytoplasms. The numerical density of the granule neurons of the dentate gyrus was decreased. CD163 immunohistochemistry showed massive microglial activation in the pyramidal sectors of the hippocampus and in the dentate gyrus (**Figure 3, a**). In the cerebellum (**Figure 3, b**), neuronal loss and microglial activation were severe in the dentate nucleus, as well as in the granular and Purkinje cell layers. The loss of Purkinje cells was complete, underlined by the hypertrophy of Bergmann glia. The neuronal loss was severe in the *substantia nigra*, *locus cœruleus* and pontine nuclei (**Supplementary Table 1**). Numerous macrophages were observed in the root of the oculomotor nerve in which axonal and myelin loss was severe (**Figure 3, e**). Nodules of neuronophagia were found in the medulla oblongata and in the anterior horns of the spinal cord (**Figure 3, c**). The spinal roots were spared.

Detection and quantification of Umbre virus sequences from patient samples

Post-mortem, metatranscriptomics identified viral sequences related to Umbre virus in the brain of patient 1 and in the brain and spinal cord of patient 2 (**Supplementary Figure 1**). Quantification of viral titer by RT-qPCR using primers derived from the sequence of Umbre virus S, M and L segments indicated approximately 10^6 to 10^8 genome copies/gram of brain for both patients. Patient 2 also tested positive, albeit less strongly, in the liver and lymph nodes with viral genome copies ranging from 10^4 to 10^6 per gram of tissue (**Supplementary Figures 2-4**). Full coding sequence of the S, L and M

segments of Umbre virus were obtained by a combination of RT-PCR and Rapid Amplification of cDNA Ends (RACE). Complete coding sequences were deposited in GenBank under accession numbers MK204828, MK204829, MK204830 (Patient 1) and MN395656, MN395657, MN395658 (Patient 2).

No CSF from patient 1 was available. Three CSF samples from patient 2, collected less than three months before death, were tested by RT-PCR for the three segments of Umbre virus and were negative. In addition, 193 CSFs from meningoencephalitis cases collected in Montpellier and Nimes, two southern cities close to the Camargue region (**see Methods in the Supplementary Material**), were tested by RT-PCR for Umbre virus S segment. None was positive.

Phylogenetic characterization of Umbre virus strains

The viral sequences found in the two patients were closely related to Umbre virus strain IG1424, isolated in India (97.6%-97.9% amino-acids identity for the L segment), and to a lesser extent to Koongol virus, isolated in Australia (70.5%-71.0% AA Id for L segment) (**Figure 4, a; Supplementary Tables 3 & 4**). According to the species demarcation criteria of the International Committee on Taxonomy of Viruses (ICTV) for orthobunyaviruses [6], the virus strain IG1424 and the two viral strains identified from the two patients belong to the same species and represent different strains of Umbre virus. We therefore gave the names Umbre orthobunyavirus strain Moissiacense (Patient 1) and Umbre orthobunyavirus strain Marna (Patient 2), in reference to the French regions where the patients lived (Moissac and Val-de-Marne, respectively).

Umbre virus infected brain neurons

In situ hybridization was performed on tissue sections from samples of frontal cortex, in which microglial activation was severe. Probes homologous to the S, M and L segments of Umbre virus were positive in the cell body and apical dendrite of pyramidal neurons in both patients (**Figure 2, f and Figure 3, f**), while glial cells, macrophages or lymphocytes were negative. Positive neurons were

scattered in case 1 but numerous in case 2. Viral sequences were not found in five biopsy and autopsy samples of control cases with encephalitis of other documented causes.

Detection and prevalence of viral sequences related to Umbre virus in Culex pipiens captured in the south of France

Umbre virus has never been described in Europe. Since this virus is borne by mosquitoes [7] we attempted to determine if it could be detected in mosquitoes captured in Camargue between 2015 and 2017 (**see Methods in the Supplementary Material**). Camargue is located between the Mediterranean Sea and the two arms of the Rhône delta. It is a touristic area, in the South of France, inhabited by many species of insects and notoriously by mosquitoes. Patient 2 stayed in Camargue during the weeks preceding the onset of her disease. Patient 1 was living 200 km west of the Rhone delta and had never travelled outside continental France. All mosquito pools were negative by RT-PCRs targeting the S, M and L segments of Umbre virus. Four pools among the 133 pools collected in 2015 were, however, positive for the L-segment of Koongol virus (**Figure 4, b**).

Serological survey

Three hundred sera from control patients and 34 sera from encephalitis cases from the South of France including the Camargue region were screened with an ELISA test that we developed to detect Umbre virus antibodies (**Supplementary Material; Supplementary Figures 5-8**). No serum gave a positive result.

Discussion

Inaccurate diagnosis of encephalitis is a main issue as immunosuppressive treatments can be deleterious in case of viral infection. Metatranscriptomics identified sequences of Umbre virus in brain samples from two immunocompromised patients with clinical and pathological signs of encephalitis. In the two cases, behavioral symptoms preceded neurological signs caused by involvement of the basal

ganglia (extrapyramidal syndrome) and of the brainstem (swallowing difficulties). There was no fever. The CSF was normal or with a mild hypercytosis. Pathologically, microglial activation, perivascular cuffing by mononucleated cells including T-lymphocytes, neuronal loss and neuronophagia ascertained the diagnosis of encephalitis. The relative scarcity of lymphocytes, contrasting with the abundance of microglial activation, and the frequency of neuronophagia were noticeable in the two cases. The changes predominated in the grey matter (cerebral cortex, striatum, cerebellar cortex and dentate nucleus). At least in case 2, there was a severe involvement of the brainstem and spinal cord. Although never isolated previously in cases of human or animal encephalitis, Umbre virus may be taken as causal in the two reported cases because of the high number of recovered genomes (around 10^8 genome copies/gram) and the demonstration that Umbre virus infected the neurons of the two patients as seen by *in situ* hybridization, a key feature of arboviruses responsible for encephalitis [8]. In addition, no other pathogen was found (**see Methods in the Supplementary Material**).

Umbre virus (genus *Orthobunyavirus*, family *Peribunyaviridae)* was first identified in *Culex sp*. mosquitoes in India in the 1950s and was catalogued as an arthropod borne (arbo-) virus after successful disease transmission experiments in mice [7]. In the 1970s, related viruses named Little Sussex and Koongol were identified in *Culex sp.* in Queensland, Australia [9,10]. The pathogenic potential, in human, of viruses related to the Umbre/Koongol group, however, remained uncertain despite that they are classified by the Center for Disease Control and Prevention (CDC) as 'Probable Arbovirus'. Serological surveys based on hemagglutination assay have suggested that members of the Umbre/Koongol group could infect several mammals, but this has not been confirmed with a more specific technique such as seroneutralization [11]. Only recently, a partially characterized orthobunyavirus closely related to Umbre virus, causing severe kidney disease in broiler chickens, has been reported in Malaysia [12]. We now report the first human cases leading to brain infection with a virus from the Umbre/Koongol group.

In this study, the origin of the two Umbre virus strains could not be elucidated. No Umbre virus could be traced by RT-PCR in pools of mosquitoes isolated in Camargue. Sequences from Koongol virus could however be identified in a small number of mosquitoes, indicating the presence of still unidentified orthobunyaviruses, close to Umbre virus, in the south of France. We concluded that the two patients were possibly infected by mosquito bites – a finding that should stimulate more comprehensive epidemiological studies of the virome of mosquitoes in this area.

Diagnosis of orthobunyavirus encephalitis is based on antibody testing [13]. Development of a seroneutralization test requires virus isolation. We were unfortunately unsuccessful in our attempts to isolate the virus in Vero cells and by intracerebral inoculation of Ag129 mice devoid of interferon receptors (not shown), which is unusual for arboviruses [14] and could explain the lack of previous identification. Alternatively, we tested the prevalence of antibodies binding the Gc head domain protein of Umbre virus in a first series of control (N=300) and encephalitis (N=34) cases but did not find any positive case. It is noteworthy that, because of the hypo- or agammaglobulinemia status of the two patients, the absence of human serum that can serve as a positive control complicated the methodology. Our observations nevertheless suggest that the prevalence of infection in the general population is low or that the virus is unable to infect most individuals with a normal immune system. The actual risk of disease transmission in immunocompromised individuals may be different and remains unknown. Immune deficit - and particularly the deficit in neutralizing antibodies [15] - may have played a crucial role in the development of the encephalitis in a way that remains to be investigated.

As for other major arboviruses, like JEV, Umbre virus seems to be hardly detectable in the CSF after the onset of the disease [16,17] (three CSFs from P2 tested negative, and none of the 193 CSFs taken from suspected cases of meningo-encephalitis in two southern cities close to the Camargue region tested positive). Similarly, negative PCR-testing of the CSF was also recorded for Cache Valley virus, another orthobunyavirus identified recently in the brain of an immunodeficient patient [18]. This

suggests that in immunodeficient patients, especially patients without circulating B cells, persistent neurological symptoms should evoke a viral encephalitis that only a brain biopsy can confirm at an early stage.

In conclusion, Umbre virus can cause encephalitis in deeply immunocompromised humans, is present in Southern Europe and could be transmitted by mosquito bites. Umbre virus should be added to targeted tests in routine diagnosis of brain tissue from encephalitis cases with unidentified etiology, in particular in a context of immune suppression. The negativity of the CSF in such cases raises the question of brain biopsy at an early stage in the management of encephalitis of unknown etiology.

Funding

This work was supported by Laboratoire d'Excellence "Integrative Biology of Emerging Infectious Diseases" (grant no. ANR-10-LABX-62-IBEID).

Acknowledgments

We thank the EID agents for their involvement in mosquito collection, IDvet (Grabels, France) for kindly provided Schmallenberg virus ELISA kits and a Schmallenberg positive control serum, and Daniel Dunia. The National network of Neuropathology for the surveillance of Creutzfeldt-Jakob disease is supported by Santé Publique France, AP-HP and the DGOS (Direction Générale de l'Offre de Soins) of the French Ministry of Health.

Disclosures

P.P., D.C., C.D., D.S., and M.E. have submitted patent application covering the findings of this work. All other authors have declared no conflict of interest.

References

1. Glaser CA, Honarmand S, Anderson LJ, et al. Beyond viruses: clinical profiles and etiologies associated with encephalitis. Clin Infect Dis Off Publ Infect Dis Soc Am **2006**; 43:1565–1577.

2. Venkatesan A, Tunkel AR, Bloch KC, et al. Case definitions, diagnostic algorithms, and priorities in encephalitis: consensus statement of the international encephalitis consortium. Clin Infect Dis Off Publ Infect Dis Soc Am **2013**; 57:1114–1128.

3. Mailles A, Stahl J-P, Bloch KC. Update and new insights in encephalitis. Clin Microbiol Infect Off Publ Eur Soc Clin Microbiol Infect Dis **2017**; 23:607–613.

4. Tabachnick WJ. Climate Change and the Arboviruses: Lessons from the Evolution of the Dengue and Yellow Fever Viruses. Annu Rev Virol **2016**; 3:125–145.

5. Ashraf U, Ye J, Ruan X, Wan S, Zhu B, Cao S. Usutu virus: an emerging flavivirus in Europe. Viruses **2015**; 7:219–238.

6. International Committee on Taxonomy of Viruses (ICTV). Available at: https://talk.ictvonline.org/ictv-reports/ictv_9th_report/

7. Dandawate CN, Rajagopalan PK, Pavri KM, Work TH. Virus isolations from mosquitoes collected in North Arcot district, Madras state, and Chittoor district, Andhra Pradesh between November 1955 and October 1957. Indian J Med Res **1969**; 57:1420–1426.

8. Salimi H, Cain MD, Klein RS. Encephalitic Arboviruses: Emergence, Clinical Presentation, and Neuropathogenesis. Neurother J Am Soc Exp Neurother **2016**; 13:514–534.

9. Doherty RL, Carley JG, Kay BH, Filippich C, Marks EN, Frazier CL. Isolation of virus strains from mosquitoes collected in Queensland, 1972-1976. Aust J Exp Biol Med Sci **1979**; 57:509–520.

10. Doherty RL, Carley JG, Mackerras MJ, Marks EN. Studies of arthropod-borne virus infections in Queensland. III. Isolation and characterization of virus strains from wild-caught mosquitoes in North Queensland. Aust J Exp Biol Med Sci **1963**; 41:17–39.

11. Shchetinin AM, Lvov DK, Deriabin PG, et al. Genetic and Phylogenetic Characterization of Tataguine and Witwatersrand Viruses and Other Orthobunyaviruses of the Anopheles A, Capim, Guamá, Koongol, Mapputta, Tete, and Turlock Serogroups. Viruses **2015**; 7:5987–6008.

12. Palya V, Kovács EW, Marton S, et al. Novel Orthobunyavirus Causing Severe Kidney Disease in Broiler Chickens, Malaysia, 2014-2017. Emerg Infect Dis **2019**; 25:1110–1117.

13. Miller A, Carchman R, Long R, Denslow SA. La Crosse viral infection in hospitalized pediatric patients in Western North Carolina. Hosp Pediatr **2012**; 2:235–242.

14. Reynolds ES, Hart CE, Hermance ME, Brining DL, Thangamani S. An Overview of Animal Models for Arthropod-Borne Viruses. Comp Med **2017**; 67:232–241.

15. Hellert J, Aebischer A, Wernike K, et al. Orthobunyavirus spike architecture and recognition by neutralizing antibodies. Nat Commun **2019**; 10:879.

16. Dubot-Pérès A, Sengvilaipaseuth O, Chanthongthip A, Newton PN, de Lamballerie X. How many patients with anti-JEV IgM in cerebrospinal fluid really have Japanese encephalitis? Lancet Infect Dis **2015**; 15:1376–1377.

17. Touch S, Hills S, Sokhal B, et al. Epidemiology and burden of disease from Japanese encephalitis in Cambodia: results from two years of sentinel surveillance. Trop Med Int Health TM IH **2009**; 14:1365–1373.

18. Wilson MR, Suan D, Duggins A, et al. A novel cause of chronic viral meningoencephalitis: Cache Valley virus. Ann Neurol **2017**; 82:105–114.

Figure 1

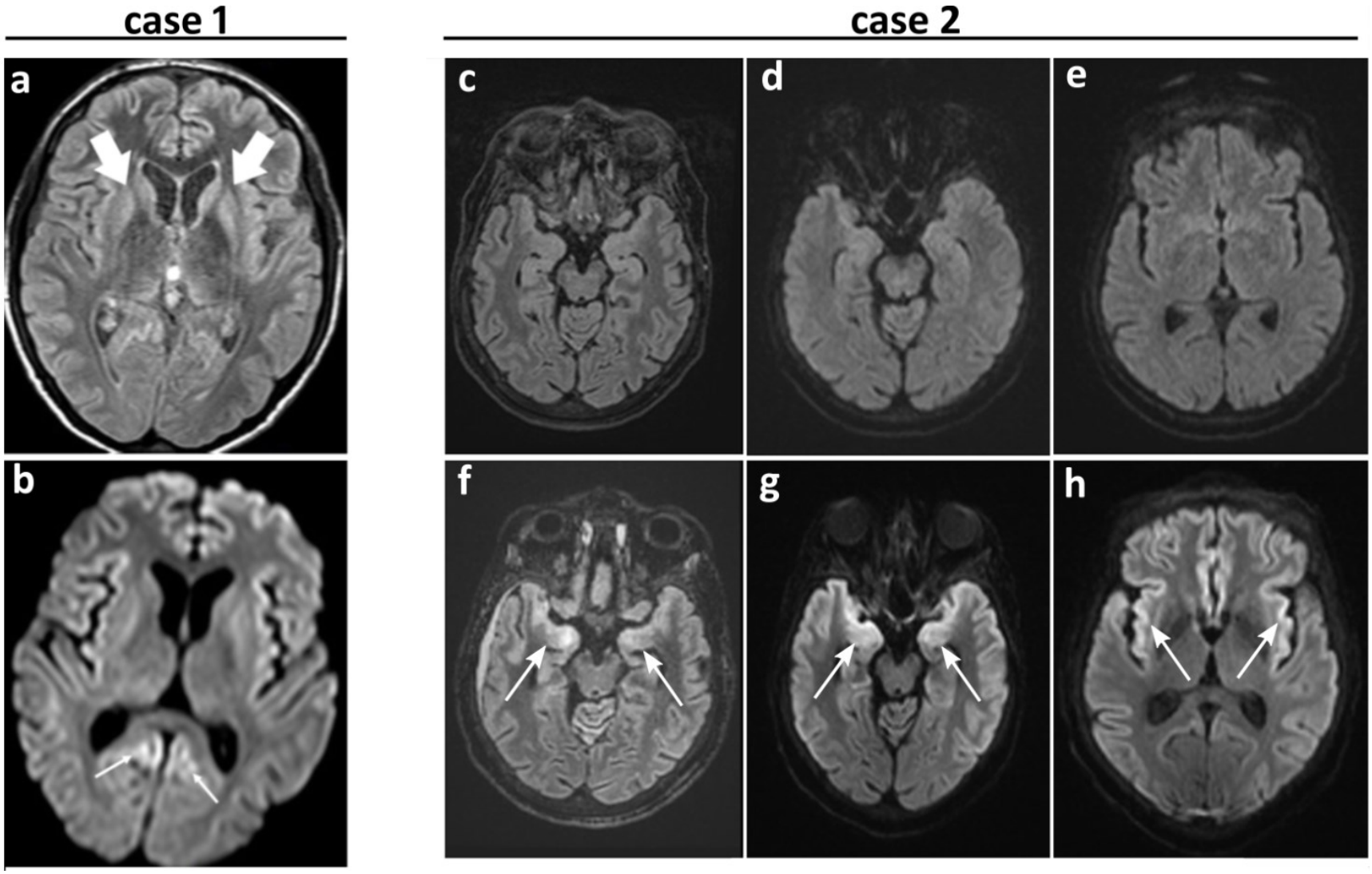

Figure 2

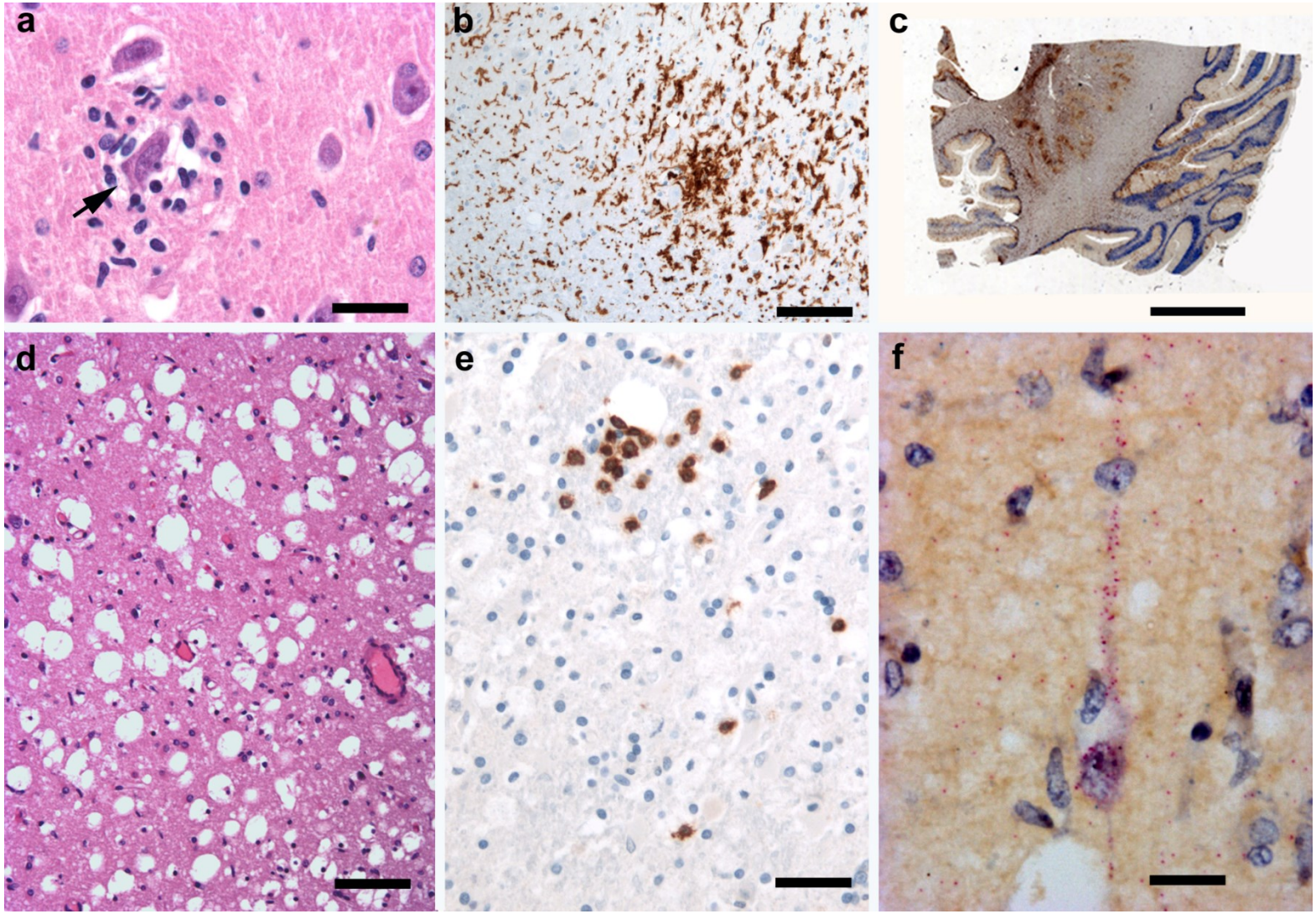

Figure 3

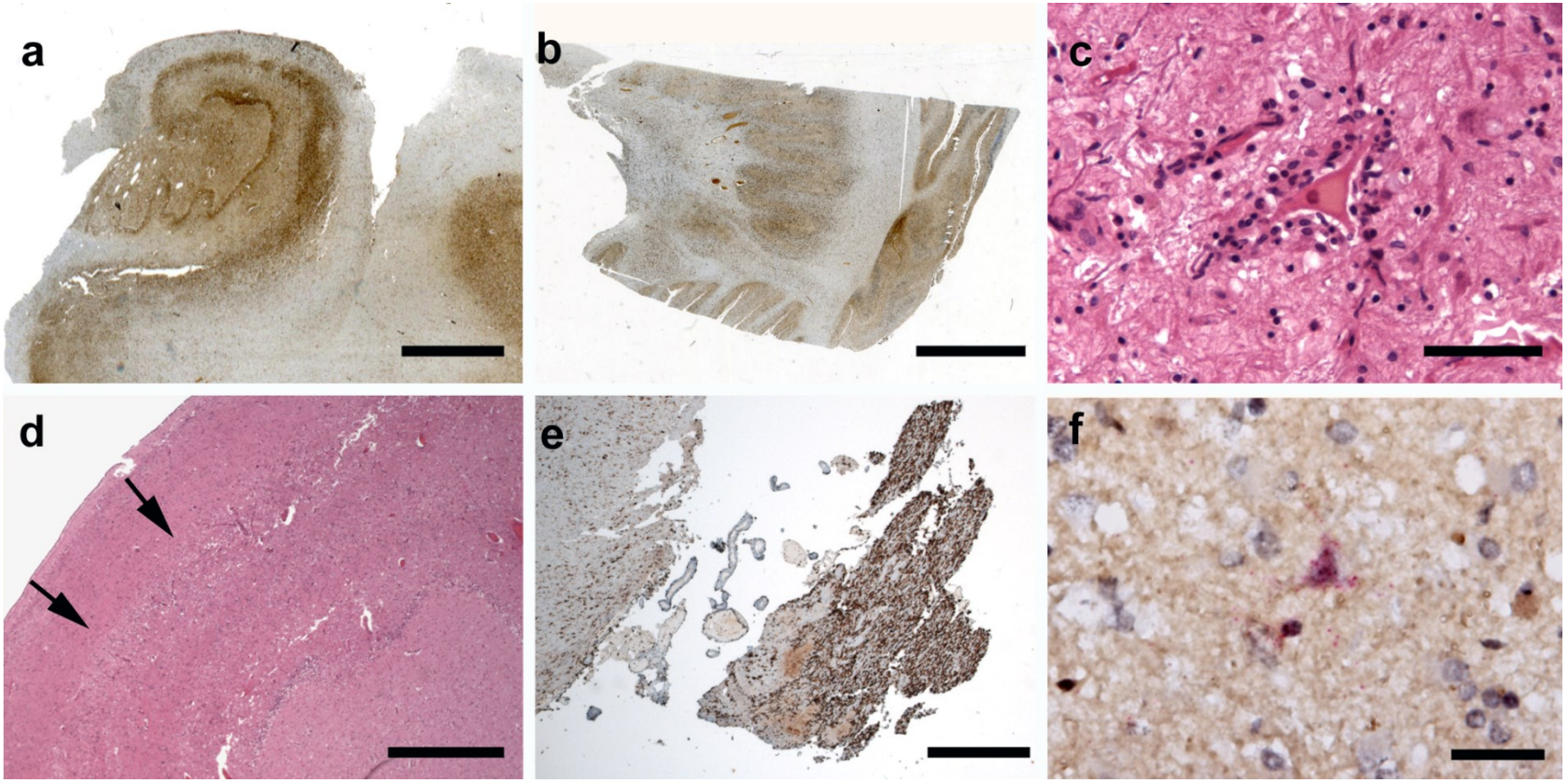

Figure 4

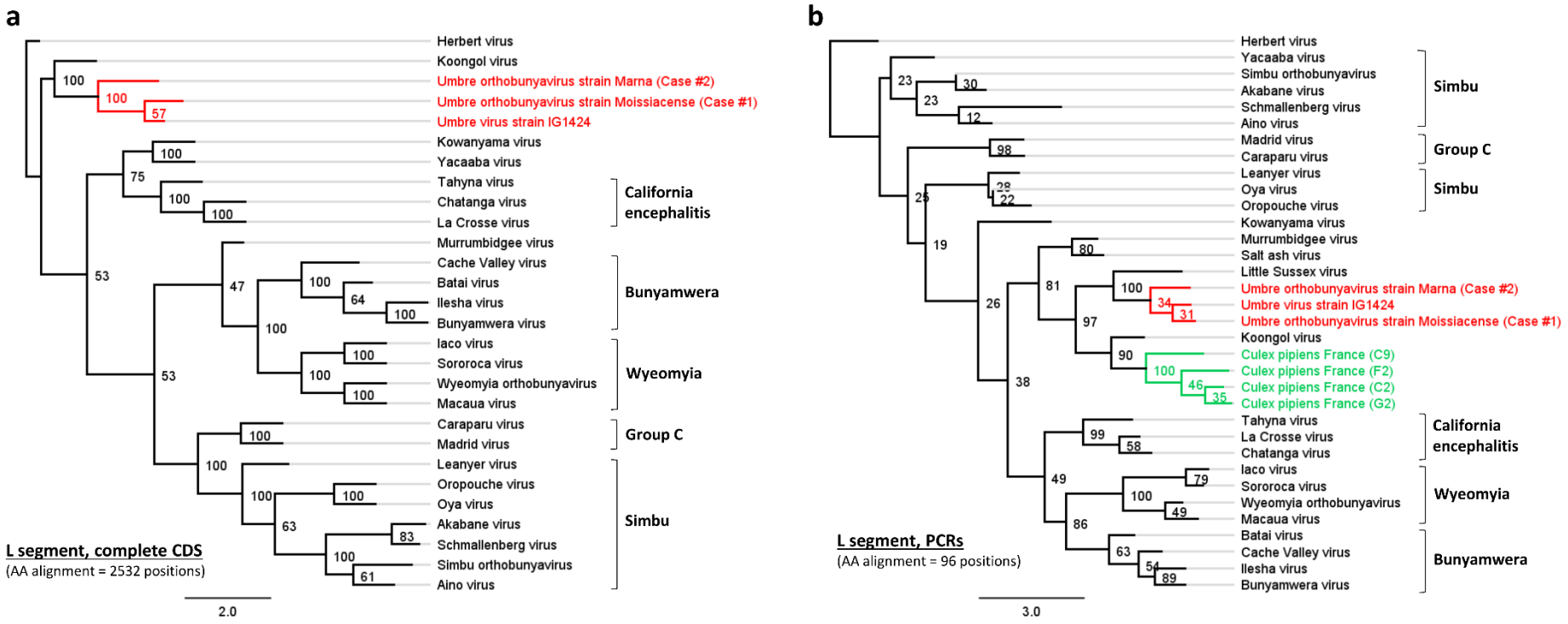
a
Herbert virus
Koongol virus
Umbre orthobunyavirus strain Marna (Case #2)
Umbre orthobunyavirus strain Moissiacense (Case #1)
Umbre virus strain IG1424
Kowanyama virus
Yacaaba virus
Tahyna virus
Chatanga virus
La Crosse virus
Murrumbidgee virus
Cache Valley virus
Batai virus
Ilesha virus
Bunyamwera virus
Iaco virus
Sororoca virus
Wyeomyia orthobunyavirus
Macaua virus
Caraparu virus
Madrid virus
Leanyer virus
Oropouche virus
Oya virus
Akabane virus
Schmallenberg virus
Simbu orthobunyavirus
Aino virus
California encephalitis
Bunyamwera
Wyeomyia
Group C
Simbu
L segment, complete CDS
(AA alignment = 2532 positions)
2.0
b
Herbert virus
Yacaaba virus
Simbu orthobunyavirus
Akabane virus
Schmallenberg virus
Aino virus
Madrid virus
Caraparu virus
Leanyer virus
Oya virus
Oropouche virus
Kowanyama virus
Murrumbidgee virus
Salt ash virus
Little Sussex virus
Umbre orthobunyavirus strain Marna (Case #2)
Umbre virus strain IG1424
Umbre orthobunyavirus strain Moissiacense (Case #1)
Koongol virus
Culex pipiens France (C9)
Culex pipiens France (F2)
Culex pipiens France (C2)
Culex pipiens France (G2)
Tahyna virus
La Crosse virus
Chatanga virus
Iaco virus
Sororoca virus
Wyeomyia orthobunyavirus
Macaua virus
Batai virus
Cache Valley virus
Ilesha virus
Bunyamwera virus
Simbu
Group C
Simbu
California encephalitis
Wyeomyia
Bunyamwera
L segment, PCRs
(AA alignment = 96 positions)
3.0

Figure legends

Figure 1: Brain MRI of the two patients with Umbre virus encephalitis

a & b: case 1. Axial FLAIR (a) and diffusion-weighted (b) images, revealing mild hyper intensity of both putamina (thick arrows), and of frontal, insular and posterior cingulate cortices (thin arrows).

c to h: case 2. Brain MRI at month 1 (c to e) and month 5 (f to h); c & f: axial T2; d & e; g & h: diffusion-weighted images. c, d, e: normal hippocampi and insular cortices at month 1. f, g, h: bilateral hypersignal (arrows) of the hippocampi and insular cortices, with mild bi-hippocampi atrophy.

Figure 2: Histopathology in case 1

a: Parahippocampal cortex. Haematein-eosin. Microglial cells surrounding a neuron (black arrow), suggesting neuronophagia.

b: Dentate nucleus. IBA-1 immunohistochemistry. Diffuse microglial activation and microglial nodule.

c: Cerebellum. CD163 immunohistochemistry. Distribution of activated microglia. Enhancement in the dentate nucleus.

d: Temporal cortex. Haematein-eosin. Spongiosis.

e: Caudate nucleus. CD3 immunohistochemistry. Clusters of T-lymphocytes.

f: Frontal cortex. In situ hybridization with a bunyavirus probe. Labeling (red) of the cell body and dendritic shaft of a pyramidal neuron.

Scale bars: a & e = 50 µm; b & d = 100 µm; c = 5 mm; f = 25 µm.

Figure 3: Histopathology in case 2

a: Right hippocampus. CD163 immunohistochemistry. Distribution of activated microglia. Enhancement of the dentate gyrus and pyramidal sectors of the cornu Ammonis.

b: Cerebellum. CD163 immunohistochemistry. Distribution of activated microglia. Enhancement in the dentate nucleus and cerebellar cortex.

c: Anterior horn of the spinal cord. Haematein-eosin. Microglial cells surrounding a neuron, suggesting neuronophagia.

d: Right hippocampus. Haematein-eosin. Neuronal loss in CA1 (black arrows).

e: Roots of the oculomotor nerve. CD163 immunohistochemistry. Infiltration by macrophages.

f: Frontal cortex. In situ hybridization with a bunyavirus probe. Labeling (red) of the cell body of a pyramidal neuron.

Scale bars: a & b = 5 mm; c = 50 µm; d = 100 µm; e = 500 µm; f = 25 µm.

Figure 4: Phylogenetic analysis of orthobunyaviruses

RAxML phylogeny of orthobunyaviruses based on the L segment with 100 bootstrap replications. a: full coding sequences. b: PCR-targeted sequences. The bootstrap values are given at each branches. Serogroups are indicated in black on the right side. Umbre virus strains are depicted in red. PCR-amplified sequences obtained from *Culex pipiens* mosquitoes captured in Camargue are highlighted in green (samples C2, F2, G2 and C9). Phylogenetic trees based on the M and S segments were congruent with the L segment and are not presented. Details on the method are available in the **Supplementary Material.**

Supplementary Material (online resource)

Identification of Umbre Orthobunyavirus as a Novel Zoonotic Virus Responsible for Lethal Encephalitis in Two French Patients with Hypogammaglobulinemia

METHODS 2
Context of the study 2
Neuropathology 2
Immunohistochemistry 2
Western Blot 3
Metatranscriptomics 3
In-situ hybridization 4
Phylogenetic analysis 5
RT-PCR 6
Serology 6
Recombinant protein preparation 6
Serum samples 7
Serological assay 8
Serological survey 8
Mosquito capture 9
CSF analysis 9
SUPPLEMENTARY FIGURES 11
Supplementary Figure 1 11
Supplementary Figure 2 12
Supplementary Figure 3 12
Supplementary Figure 4 13
Supplementary Figure 5 13
Supplementary Figure 6 14
Supplementary Figure 7 14
Supplementary Figure 8 15
SUPPLEMENTARY TABLES 16
Supplementary Table 1 16
Supplementary Table 2 17
Supplementary Table 3 18
Supplementary Table 4 19
REFERENCES 20

METHODS

Context of the study

The two cases presented in this study were selected from a larger series of sixty brain samples collected either from autopsy or biopsy, with brain inflammation, in which we performed a molecular screening for the presence of pathogens. Over a period of 2 years, seventeen of these samples were analyzed by high-throughput sequencing with a metatranscriptomics approach. Patient #2 had undergone a brain biopsy followed 10 days later by a diagnostic autopsy. Patient #1 had been included in the National Creutzfeldt-Jakob disease (CJD) surveillance network, coordinated by the neuropathology department of Pitié-Salpêtrière. This network collects the postmortem samples from all cases in France with a diagnosis of "possible" or "likely" CJD, according to the World Health Organization criteria (WHO Recommended surveillance standards WHO/CDS/CSR/99.2). The aim of this network is not only to confirm CJD but also to identify differential diagnoses in cases of rapidly progressive neurological diseases. In a large series of 1572 cases autopsied between 1992 and 2009 we found that 30 % of the collected cases were not prion diseases [1].

Neuropathology

The biopsy sample was left overnight in formalin (10% of the commercial formalin solution containing 4% formaldehyde). After autopsy, fresh brain slices were stored frozen at -80°C prior to nucleic acid extraction. The whole brains were immersion-fixed in formalin 10%. In case 1, only 9 samples were available. In case 2, a systematic protocol was applied. Samples of cerebral neocortex and hippocampus, basal ganglia, brainstem, cerebellum and spinal cord were analyzed.

Immunohistochemistry

The samples were paraffin–embedded. Three µm thick sections were obtained and stained with haematein-eosin, Periodic Acid Schiff (PAS) and Luxol Fast Blue. Immunochemistry was performed with

various primary antibodies (**Supplementary Table 2**) using a Ventana Ultra Stainer (Roche) with diaminobenzidine as chromogen. Immunohistochemistry was performed independently for the two patients.

Western Blot

The search for PrPres was performed in the two cases by Western blot according to published protocols [2].

Metatranscriptomics

By using untargeted metatranscriptomics, we aimed at identify RNA sequences from bacteria, fungi, viruses or protozoans without prior hypothesis on the involved pathogen. RNA, rather than DNA, is indicative of living microorganisms. For each patient individually, grinding of the *post-mortem* frozen tissues was performed with a tissue homogenizer (Bertin) based on a bead beating technology. Total RNA was isolated with the Trizol procedure, followed by DNAse treatment (Qiagen) and purification using RNeasy spin columns (Qiagen). RNA Integrity Number (RIN) ranged between 2.9 and 6.9 after extraction, with 18S and 28S rRNA peaks visible. For each sample, a cDNA library was constructed with the SMARTer Stranded Total RNA-Seq Kit - Pico Input Mammalian (Takara Bio, kit v.1 for patient 1 and v.2 for patient 2). The llibraries of the 2 patients were made independently. The procedure included a random reverse transcription of total RNA into first strand cDNA, a depletion of human ribosomal cDNA, and a final PCR amplification. The cDNA libraries were sequenced independently for the two patients in 1x150bp on a NextSeq500 instrument (Illumina) using High Output flow cells, generating between 35 and 116 million reads (**Supplementary Figure 1, A**). A set of reference human transcripts was used as an internal positive control (**Supplementary Figure 1, B**). We have not sequenced the ante-mortem biopsy of Patient #2. The vast majority of raw reads had quality scores (Q scores) above 20. Raw reads were trimmed to remove low quality bases and sequencing adapters at their ends with AlienTrimmer [3] (version 0.4.0, options -k 10 -m 5 -l 50 -p 80 -c 012 -q 20). The reads were then assembled with MegaHit [4] (version 1.1.2, with default options). Unassembled reads were kept as singletons. Resulting

sequences were aligned after translation in all the six possible reading frames (3 by DNA strand) against a viral protein reference comprehensive database we have developed (RVDB [5]) using the DIAMOND [6] program. Matches with viral sequences were controlled in NCBI NR protein and NCBI NT databases to identify and eliminate false positives. The identification of a virus, previously known or still to be described, was based on these aligned protein sequences. The search for bacteria, fungi and protozoans sequences was done with Kraken2 [7], Centrifuge [8] and MethaPhlAn2 [9].

In-situ hybridization

ViewRNA ISH Tissue Assay Kit 2-plex (Thermo Fisher Scientific) was used to detect RNA sequences. According to the manufacturer, the technique has a sensitivity of one single copy and is based on branched DNA technology. ViewRNA Probes have a double Z configuration: one side of the Z is complementary to the target sequence and its other side is complementary to the pre-amplifier DNA sequence. A cocktail of 95 custom bDNA probes was designed to target the 3 genomic segments of Umbre orthobunyavirus strain Moissiacense (15 probes for segment S, 40 probes for segment M, 40 probes for segment L) and was revealed (as the “probe type 1” of the kit) by a red signal. A mix of control probes targeting human GAPDH, ACTB and PPI transcripts was revealed (as the “probe type 6” of the kit) by a blue signal. To unmask RNA targets, the tissue sections (after deparaffinization by xylene and ethanol) were pretreated by heating at 95°C during 20 min in PBS 1X, cooling at room temperature (RT) during 5 min, washing 2 x 1 min in distilled water, washing 1 min in PBS 1X, protease digestion during 10 min at 40°C in a hybridizer Denaturation & Hybridization System (NB-12-0001, Neobrite), and washing 2 x 1 minute in PBS at room temperature (RT). Tissue sections were fixed 5 min in formaldehyde 4% at RT, then washed 2 x 1 min in PBS 1X. Probes diluted in Probe Set Diluant QT (ThermoFisher) - a proprietary aqueous solution containing formamide, detergent, and blocker- were added on the tissue section and were hybridized during 2 hours at 40°C in the hybridizer. The sections were washed 3 x 2 min in Wash Buffer. During the amplification step, sections were incubated 25 min at 40°C in PreAmplifier Mix containing the PreAmplifier DNA type 1 and type 6, washed 3 x 2 min in Wash Buffer, incubated 15 min

at 40°C in Amplifier Mix containing the Amplifier DNA type 1 and type 6, and washed 3 x 2 min. In order to produce the blue signals, the section were incubated with 6-AP (an alkaline phosphatase binding the amplifier DNA type 6) during 15 min at 40°C in the hybridizer, washed 3 x 3 min in Wash Buffer, incubated with Fast Blue solution during 30 min at RT, and washed 3 x 3 min in Wash Buffer. The 6-AP was quenched by AP STOP QT during 30 min at RT. In order to produce the red signals, the section were incubated with 1-AP (an alkaline phosphatase binding the amplifier DNA type 1) during 15 min at 40°C in the hybridizer, washed 3 x 3 min in Wash Buffer, incubated with Fast Red solution during 45 min at 40°C in the hybridizer, and washed 1 min in PBS. Haematoxylin was used for counterstaining. *In-situ* hybridization was performed at different times for the two patients, with Patient #1 having secondarily served as a positive control for Patient #2. The five negative controls used for ISH were other encephalitis cases coming from the larger series of brain samples (see section "Context of the study") that have been sequenced with a comparable sequencing depth and that were either negative (3/5) or positive for viruses other than Umbre (2/5).

Phylogenetic analysis

Alignments of amino acids sequences were done with MAFFT v7.388 [10,11] and manually adjusted when needed. Identity matrices are given in **Supplementary Table 3 and Supplementary Table 4**. RAxML phylogeny with 100 bootstrap replications was performed in Geneious 11.1.5 [12] after initial model selection done in MEGA7 [13]. Only complete CDS sequences were kept for phylogenetic analysis. Herbert virus (Family: *Peribunyaviridae*; Genus: ***Herbevirus***) was used as outgroup. Accession numbers for L segment: Aino virus (NC_018465.1), Akabane virus (NC_009894.1), Batai virus (JX846606.1), Bunyamwera virus (NC_001925.1), Cache Valley virus (KC436106.1), Caraparu virus (KF254793.1), Chatanga virus (EU616903.1), Herbert herbevirus (NC_038714.1), Iaco virus (JN572065.1), Ilesha virus (KF234075.1), Koongol virus (KP792669.1), Kowanyama virus (KT820202.1), La Crosse virus (NC_004108.1), Leanyer virus (HM627178.1), Little Sussex virus (KT720483.1), Macaua virus (JN572068.1), Madrid virus (KF254779.1), Murrumbidgee virus (KF234253.1), Oropouche virus

(NC_005776.1), Oya virus (JX983194.1), Salt ash virus (KF234256.1), Schmallenberg virus (NC_043583.1), Simbu orthobunyavirus (HE795108.1), Sororoca virus (JN572071.1), Tahyna virus (HM036219.1), Umbre virus strain IG1424 (KP792687.1), Umbre orthobunyavirus strain Marna (MN395656), Umbre orthobunyavirus strain Moissiacense (MK204828), Wyeomyia orthobunyavirus (JN572080.1), Yacaaba virus (KT820208.1).

RT-PCR

RT-PCRs were done on the exact same tissue RNA extracts that were used for sequencing. Reverse transcription reactions were performed using the SuperScript IV First-Strand Synthesis System (Thermo Fischer Scientific). Quantitative PCR were done in SYBR Green format with 45 cycles of amplification. Human beta-actin was included in the RT-PCR experiments as a positive control of the cDNA. No Template Control (NTC) wells, validating the absence of cDNA or DNA contaminant into the PCR mix, were also added to the experiment. Positive amplicons after 45 cycles were purified on gel and serial-dilutions were made to generate standard curves (**Supplementary Figures 2-4**). Primer pairs used for detection of Umbre virus were: L segment AGAATTGGTTATCCCAGATGAGGT (forward) and GCCATAAATTGAAAATGGTTCTCCA (reverse); M segment ACAGGRCAAATAGCACTAAAGGT (forward) and CCTTCRTCTCTCACTTTGCAG (reverse); S segment AAACGCAGAACTGGGTAGCA (forward) and GAGTTAGCTCATCGTCCGCA (reverse). The primer pair used for detection of the Koongol virus L segment was GACCCAATACTGTAAACAG (forward) and CGTCAGAATGCACCATTG (reverse). PCR performed after omitting the reverse transcription step for samples C2, F2, G2 and C9 were negative, supporting the detection of viral RNA rather than endogenous viral DNA in mosquitoes.

Serology

Recombinant protein preparation

The Gc head domains of Umbre orthobunyavirus strain Moissiacense (residues G477-D730 of the polyprotein precursor) and Schmallenberg virus (residues Q465-I702 of the polyprotein precursor) carrying a C-terminal Strep-tag (GGWSHPQFEK) were produced in recombinant Drosophila S2 cells (Gibco) grown at 28°C in HyClone SFM4Insect medium with L-glutamine (GE Healthcare) supplemented with 25 U/mL penicillin/streptomycin (Gibco). For this purpose, a codon-optimized synthetic gene fragment (Invitrogen) was cloned into the pMT expression vector (Invitrogen) downstream of a BiP secretion signal. The expression plasmid was co-transfected with the selection plasmid pCoPURO [14] at a mass ratio of 20:1 using the Effectene transfection reagent (Qiagen) according to the manufacturer's instructions. A polyclonal stable S2 cell line was established by selection with 7.5 µg/mL puromycin (Invivogen), which was added to the medium starting 40 h after transfection. The culture was expanded to 1 L of 10^7 cells/mL in Erlenmeyer flasks shaking at 100 rpm and at 28°C. Recombinant protein expression was then induced with 500 µM $CuSO_4$. The cell supernatant was harvested 1 week after induction, concentrated to 50 mL on a 10 kDa MWCO PES membrane (Sartorius), pH-adjusted with 0.1M Tris-Cl pH 8.0, cleared from biotin with 15 µg/mL avidin, cleared from precipitate by centrifugation at 4000 x g for 15 min at 8°C, and was used for affinity purification on a 5 mL Strep-Tactin Superflow hc column (iba Life Science). The protein was further purified by gel permeation chromatography on a HiLoad Superdex 200 pg column (GE Healthcare) in 20 mM Tris-Cl pH 8.0, 150 mM NaCl. Aliquots were flash-frozen on liquid nitrogen and stored at -80°C.

Serum samples

Three hundred serum samples randomly collected from patients attending the Montpellier University hospital as part of a collection for seroepidemiological investigation through the Arbosud project (Montpellier University MUSE project) were screened. Additional 34 serum samples from patients with diagnosis of meningitis or meningo-encephalitis were also tested (Institutional review board 2019-IRB-MPT-05-06).

Serological assay

Two in-house enzyme linked immuno assays were set up with two recombinant antigens, corresponding to the head domain of the Gc protein for respectively the Umbre virus Moissiacence strain and the Schmallenberg virus used as a negative control. Reactivity of every serum samples was concomitantly tested against each antigen in 96 wells plates. Plates were coated overnight at 4°C with 100µL of 2 µg/mL of the respective antigens. Plates were subsequently washed 3 times with PBS-tween 0.1% and further blocked with PBS-tween 0.01% plus 2% of bovine serum albumin during 2 hours at room temperature. Plates were washed 3 times before 100 µL of a one hundred dilution of serum samples in blocking solution was added. Serum samples were incubated 3 hours at room temperature. Horseradish peroxidase secondary antibody diluted in blocking solution was added after 3 washes and incubated one hour at 37°C, under agitation. TMB substrate was added and plates remained in dark at room temperature for 20 min before reaction was further stopped with H_2SO_4. The 450nm optical densities were recorded for each sample. Samples giving the highest values were alternatively tested through a commercial pan-species ELISA Schmallenberg virus assay that displays the N protein as targeted antigen, following the manufacturer recommendations (ID Screen Schmallenberg virus indirect Multi-species, IDvet, France).

Serological survey

The Gc head domain of Schmallenberg virus, an orthobunyavirus of ruminants belonging to the Simbu serogroup, served as a negative control. It was not possible to use the sera of the two Umbre patients as a positive control because of their immunoglobulin deficiency. A positive control was used for the Schmallenberg virus antigen (Schmallenberg positive reference serum kindly provided by IDVet) and was tested undiluted and at a 10-fold dilution. Three hundred sera from control patients (the control group) and 34 sera from encephalitis cases (the encephalitis group) were screened. In the control group (N=300), optical densities ranged from 0 to 4 for both antigens (**Supplementary Figure 5**). Because no

human cases of Schmallenberg virus infection have been reported [15,16], we verified and confirmed the absence of detectable antibodies against the immunodominant nucleocapsid N protein of Schmallenberg virus for samples with the highest densities, using a reference veterinary kit which included a positive control (ID Screen Schmallenberg virus indirect Multi-species, IDvet, France, data not shown). Since the Gc head domains of Schmallenberg virus and Umbre virus were designed in an orthologous manner and produced under strictly identical conditions, we concluded that optical densities values up to 4 corresponded to background noise. In the encephalitis group (N=34), all optical values were inferior to 3 (**Supplementary Figure 7**). The observed statistical differences were therefore attributed to random background noise and it was concluded that no specific antibody response was recorded.

Mosquito capture

Approximately 4,000 *Culex pipiens* female mosquitoes were captured in 2015 in the French Rhône Delta region. Mosquito capture was carried for a 24-hour period once a week between June and September. Captures were carried out in the 6 sites in parallel the same days. The June-September period covers most of the mosquito season in the study region. The population of Culex pipiens is generally rather low before or after this period (usually less than 10 females per catch). In addition, this period was selected because it includes the population peak for Culex pipiens (usually June-July depending on the site) and the peak of prevalence in mosquitoes and clinical cases in vertebrates for Culex-borne arboviruses in the region (i.e. September for West Nile and Usutu viruses, e.g. Eiden et al. 2018 [17]). 133 pools of approximately 30 individuals were made. In addition, around 100 *Culex pipiens,* 30 *Culex Sp.*, 100 *Aedes caspius*, 50 *Aedes detritus*, 10 *Aedes vexans*, 10 *Aedes Sp.*, and 20 *Anopheles* mosquitoes were captured in 2017 in Camargue and Languedoc (Southern France) and species-specific pools of 5-20 individuals were made. Of the mosquitoes captured in 2017, no positivity was recorded.

CSF analysis

RNA extracts from 193 CSFs collected in patients (attending both University hospitals of Montpellier and Nimes, two towns close to the Camargue region) presenting with a meningitis or meningo-encephalitis during the course of a regional arbovirus surveillance program during the peak mosquito activity period from 1st May to 31 November 2016 and 2017 were tested by RT-PCR using primers specific for the S segment of Umbre virus. These 193 CSFs have not been analyzed with the serological assay due to insufficient quantity remaining after RT-PCR.

SUPPLEMENTARY FIGURES

Supplementary Figure 1: Identification of Umbre virus by NGS. **(A)** Read mapping using bowtie2 [18] (v2.2.6, sensitive local mode) to Umbre virus strain IG1424 accession numbers KP792686.1 (S segment), KP792686.1 (M segment) and KP792687.1 (L segment). Red: number of reads mapped to Umbre virus. Blue: horizontal coverage (%). Green: vertical coverage (x, average value). **(B)** Read mapping to a set of reference human transcripts (internal positive control).

A

			Mapping with bowtie 2 (v2.2.6, --sensitive-local)		
Patient (Case #)	**Sample**	**Number of raw reads (10^6)**	**Umbre virus L segment (ORF)**	**Umbre virus M segment (ORF)**	**Umbre virus S segment (ORF)**
1	Brain (frontal cortex)	116.8	133 30.1% 2x	139 27.2% 4x	291 93.1% 44x
2	Brain (frontal cortex)	40.1	711 81,7% 13x	209 51,2% 6x	1,109 100,0% 173x
2	Spinal cord (cervical)	35.1	249 60,2% 4x	260 50,3% 7x	504 99,7% 77x
2	Spinal cord (thoracic)	37.9	778 84,1% 14x	903 78,9% 27x	1,433 100,0% 215x

B

			Patient 1		Patient 2					
			Brain (frontal cortex)		Brain (frontal cortex)		Spinal cord (cervical)		Spinal cord (thoracic)	
Human transcripts	**sequence id**	**sequence length (bp)**	**nb of mapped reads**	**Horizontal coverage (%)**	**nb of mapped reads**	**Horizontal coverage (%)**	**nb of mapped reads**	**Horizontal coverage (%)**	**nb of mapped reads**	**Horizontal coverage (%)**
Homo sapiens actin, beta (ACTB), mRNA	*NM_001101*	1852	52411	100.0	40550	99.1	42774	100.0	40303	100.0
Homo sapiens glyceraldehyde-3-phosphate dehydrogenase (GAPDH), transcript variant 1, mRNA	*NM_002046*	1421	21911	99.2	14428	91.6	24496	94.1	33130	95.4
Homo sapiens ribosomal protein lateral stalk subunit P0 (RPLP0), transcript variant 1, mRNA	*NM_001002*	1229	2258	92.3	4309	91.4	4621	87.9	5755	90.5
Homo sapiens neuronal cell adhesion molecule (NRCAM), transcript variant 2, mRNA	*NM_005010*	6322	8228	99.7	1793	96.3	2372	98.3	1851	97.6
Homo sapiens integrin subunit beta 2 (ITGB2), transcript variant 1, mRNA	*NM_000211*	2807	654	93.6	2580	99.2	2695	99.5	1906	99.2

Supplementary Figure 2: Quantification of Umbre virus S segment by RT-qPCR

Standard curve

	Copy number / µL	Log(copy number)	Ct
Dil. 3	1.41E+09	9.1E+00	3.31
Dil. 4	2.81E+08	8.4E+00	6.03
Dil. 5	5.63E+07	7.8E+00	8.78
Dil. 6	1.13E+07	7.1E+00	11.13
Dil. 7	2.25E+06	6.4E+00	13.73
Dil. 8	4.50E+05	5.7E+00	15.97
Dil. 9	9.00E+04	5.0E+00	20.51
Dil. 10	1.80E+04	4.3E+00	23.27
Dil. 11	3.60E+03	3.6E+00	25.08

a	-3.9844	**PCR efficiency**	1.78
b	39.512		

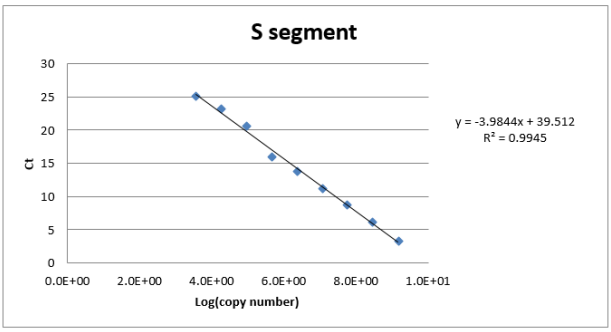

Quantification

Patient (Case #)	Sample	Ct	Copy number in PCR reaction	Copy number per gram of tissue
1	Brain (frontal cortex)	22.6	1.76E+04	1.48E+08
2	Brain (frontal cortex)	22.9	1.48E+04	6.20E+08
2	Spinal cord (cervical)	24.0	7.69E+03	3.23E+08
2	Spinal cord (thoracic)	22.4	2.03E+04	4.26E+08
2	Liver	29.6	3.04E+02	2.13E+06
2	Lymph node	31.5	1.01E+02	2.13E+06

Supplementary Figure 3: Quantification of Umbre virus M segment by RT-qPCR

Standard curve

	Copy number / µL	Log(copy number)	Ct	
Dil. 3	5.85E+08	8.8E+00	7.48	
Dil. 4	1.17E+08	8.1E+00	10.14	
Dil. 5	2.34E+07	7.4E+00	12.27	
Dil. 6	4.68E+06	6.7E+00	29.59	Removed
Dil. 7	9.36E+05	6.0E+00	18.41	
Dil. 8	1.87E+05	5.3E+00	21.41	
Dil. 9	3.74E+04	4.6E+00	24.36	
Dil. 10	7.49E+03	3.9E+00	26.62	
Dil. 11	1.50E+03	3.2E+00	29.82	

a	-4.0235	**PCR efficiency**	1.77
b	42.488		

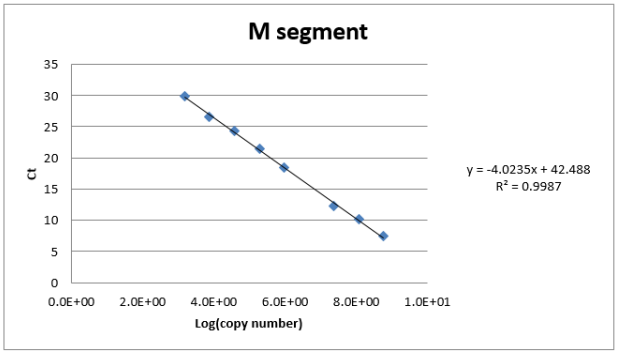

Quantification

Patient (Case #)	Sample	Ct	Copy number in PCR reaction	Copy number per gram of tissue
1	Brain (frontal cortex)	29.8	1.39E+03	1.17E+07
2	Brain (frontal cortex)	30.0	1.28E+03	5.36E+07
2	Spinal cord (cervical)	30.2	1.13E+03	4.76E+07
2	Spinal cord (thoracic)	27.9	4.20E+03	8.82E+07
2	Liver	35.5	5.33E+01	3.73E+05
2	Lymph node	36.5	3.10E+01	6.50E+05

Supplementary Figure 4: Quantification of Umbre virus L segment by RT-qPCR

Standard curve

	Copy number / µL	Log(copy number)	Ct
Dil. 3	9.65E+08	9.0E+00	6.51
Dil. 4	1.93E+08	8.3E+00	9.31
Dil. 5	3.86E+07	7.6E+00	12.05
Dil. 6	7.72E+06	6.9E+00	15.06
Dil. 7	1.54E+06	6.2E+00	18.66
Dil. 8	3.09E+05	5.5E+00	21.73
Dil. 9	6.17E+04	4.8E+00	23.88
Dil. 10	1.23E+04	4.1E+00	26.59
Dil. 11	2.47E+03	3.4E+00	28.66

a	-4.0719	**PCR efficiency**	1.76
b	43.249		

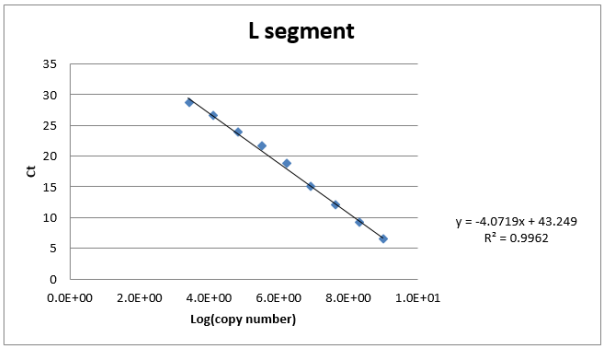

Quantification

Patient (Case #)	Sample	Ct	Copy number in PCR reaction	Copy number per gram of tissue
1	Brain (frontal cortex)	29.6	2.24E+03	1.88E+07
2	Brain (frontal cortex)	35.2	9.32E+01	3.91E+06
2	Spinal cord (cervical)	35.0	1.09E+02	4.59E+06
2	Spinal cord (thoracic)	34.0	1.92E+02	4.04E+06
2	Liver	40.5	4.76E+00	3.33E+04
2	Lymph node	neg	neg	/

Supplementary Figure 5: Distribution of raw optical density values (ELISA immunoassay) using the Gc Head domain of Schmallenberg virus and Umbre virus as antigen on a control population (N=300). Black triangle: Schmallenberg positive serum tested undiluted. Small black triangle: Schmallenberg positive serum tested at a 10-fold dilution.

P value (t test) = 0.0176

How big is the difference?	
Mean ± SEM of column A	0.1869 ± 0.02598, n=300
Mean ± SEM of column B	0.2768 ± 0.02745, n=300
Difference between means	0.08998 ± 0.03779

P value (F test) = 0.3414

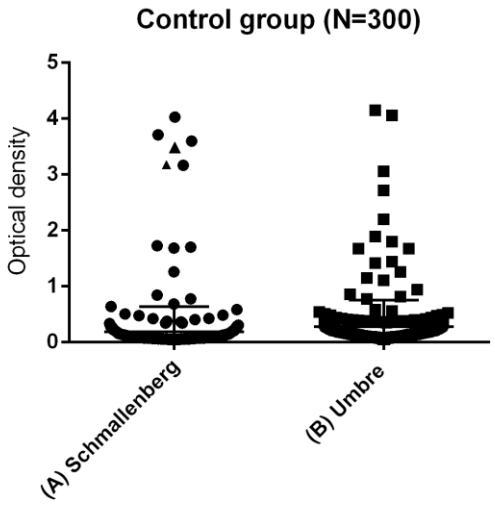

Supplementary Figure 6: XY plot of raw optical density values (ELISA immunoassay) using the Gc Head domain of Schmallenberg virus (X) and Umbre virus (Y) as antigen on a control population (N=300).

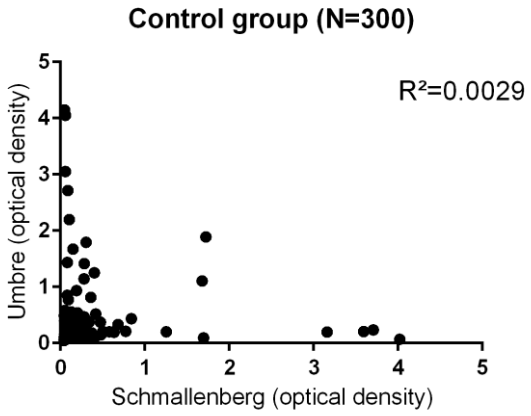

Note that absorbances up to 4 can be obtained independently without any correlation for the Umbre and Schmallenberg Gc antigens. Lack of anti-N responses for the sera showing the highest responses against Schmallenberg Gc lead us to the conclusion that such anti-Gc responses were nonspecific for both antigens.

Supplementary Figure 7: Distribution of raw optical density values (ELISA immunoassay) using the Gc Head domain of Schmallenberg virus and Umbre virus as antigen on a encephalitis group (N=34).

Black triangle: Schmallenberg positive serum tested undiluted. Small black triangle: Schmallenberg positive serum tested at a 10-fold dilution.

P value (t test) = 0.0006

How big is the difference?	
Mean ± SEM of column A	0.2079 ± 0.05054, n=34
Mean ± SEM of column B	0.6435 ± 0.1104, n=34
Difference between means	0.4355 ± 0.1214

P value (F test) < 0.0001

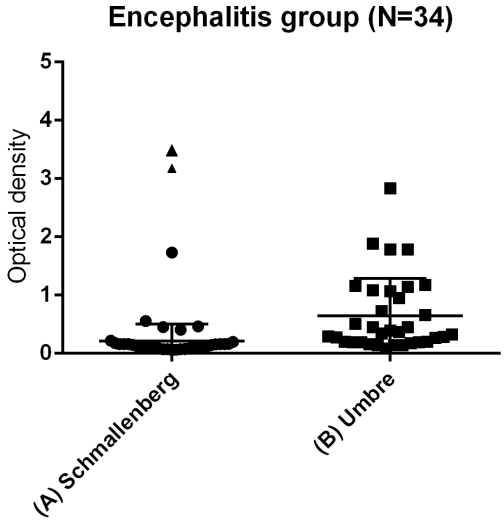

Supplementary Figure 8: XY plot of raw optical density values (ELISA immunoassay) using the Gc Head domain of Schmallenberg virus (X) and Umbre virus (Y) as antigen on a encephalitis group (N=34).

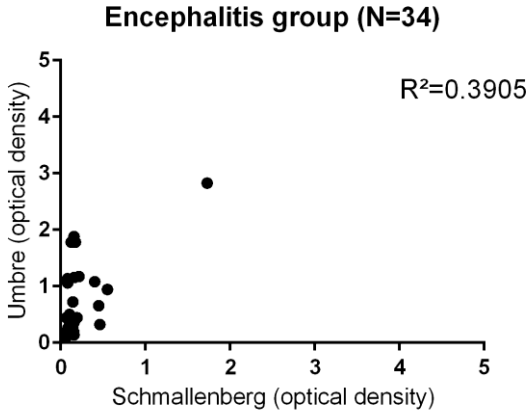

SUPPLEMENTARY TABLES

Supplementary Table 1**:** Semi-quantitative analysis of the brain lesions in cases 1 and 2

Case 1	**Neuronal loss**	**Spongiosis**	**Astrogliosis**	**Diffuse microglial activation**	**Neuronophagia**	**Lymphocytic perivascular infiltrates**
Frontal cortex	+++	+++	+++	+++	0	+
Caudate nucleus	+++	+++	+++	+++	+	+
Anterior thalamus	+	0	++	++	+	+
Posterior thalamus	+	+	+	+	++	++
Temporal cortex	++	+++	+	+	+	+
Parietal cortex	++	+++	+++	+++	0	+
Occipital cortex	+	++	+++	++	0	+
Cerebellum	+++	++	++	++	+	+
Leptomeninges	-	-	-	+	-	+
Case 2						
Frontal cortex	+++	++	+++	+++	0	+
Caudate nucleus	+++	0	+++	+++	0	++
Thalamus	+	0	+	+	0	+
Temporal cortex	+++	+	+++	+++	0	0
Parietal cortex	+	+	+++	+++	0	+
Occipital cortex	+	+	+++	+++	0	+
Cerebellum	+++	+++ (status spongiosus)	+++	+++	+	+
Mesencephalon	++	0	++	+++	+	++
Substantia nigra	+++	0	++	+++	+	+
Pons	+	0	++	++	+	+
Locus coeruleus	+++	0	++	+++	0	+
Medulla	++	0	++	++	++	+
Spinal cord	++	0	+	++	+++	0
Spinal ganglia	0	0	0	+	+	0
Spinal roots	-	-	-	+	-	0
Oculomotor nerve (III) extra-axial	-	-	-	+++	-	0
Leptomeninges	-	-	-	++ (macrophages)	-	+

Supplementary Table 2: Immunohistochemical methods

Antigen	Poly/monoclonal	Company	Immunogen	Clone	Pretreatment	Dilution	Incubation
CD3	Monoclonal (rabbit)	Roche®	nonglycosylated ε chain of human CD3	2GV6	CC1® 36 min at 95°C	Prediluted	32 min at 37°C
CD4	Monoclonal (mouse)	Dako®	External domain of CD4	4B12	CC1® 36 min at 95°C	1/40	60 min at 37°C
CD8	Monoclonal (mouse)	Dako®	13 C-terminal amino-acids of cytoplasmic domain of human CD8α	C8/144B	CC1® 36 min at 95°C	Prediluted (FLEX RTU)	32 min at 37°C
CD20	Monoclonal (mouse)	Dako®	B lymphocytes of human amygdala	L26	CC1® 36 min at 95°C	1/100	32 min at 37°C
CD68	Monoclonal (mouse)	Dako®	Subcellular fraction of human alveolar macrophages	KP1	CC1® 36 min at 95°C	1/1000	20 min at 37°C
CD163	Monoclonal (mouse)	Roche®	acute phase-regulated monocytic transmembrane protein	MRQ-26	CC1® 64 min at 95°C	Prediluted	32 min at 37°C
IBA-1	Polyclonal (rabbit)	Wako®	calcium-binding protein expressed in macrophage/microglia	_	CC1® 64 min at 95°C	1/500	32 min at 37°C
PrP	Monoclonal (mouse)	Bertin®		12F10	Formic acid 3 min + pressure canner	1/200	60 min at 37°C

CC1, a proprietary high pH (=8) buffer

Supplementary Table 3: Amino acids identity matrix on the L segment (alignment size: 2532 AA). See accession numbers in “Phylogenetic analysis”.

	Aino virus	Akabane virus	Schmallenberg virus	Simbu orthobunyavirus	Oropouche virus	Oya virus	Leanyer virus	Caraparu virus	Madrid virus	Batai virus	Bunyamwera virus	Ilesha virus	Cache Valley virus	Iaco virus	Sororoca virus	Macaua virus	Wyeomyia orthobunyavirus	Chatanga virus	La Crosse virus	Tahyna virus	Kowanyama virus	Yacaaba virus	Koongol virus	Umbre orthobunyavirus strain Marna (Case #2)	Umbre orthobunyavirus strain Moissiacense (Case #1)	Umbre virus strain IG1424	Murrumbidgee virus	Herbert virus
Aino virus		68.0	68.8	71.1	58.7	57.9	55.3	49.6	49.7	48.3	48.8	47.7	48.6	49.0	48.1	48.5	47.8	49.4	49.2	49.4	47.8	49.4	45.3	44.1	44.2	44.0	45.5	24.5
Akabane virus	68.0		70.9	70.1	58.4	57.5	54.3	50.6	50.6	48.8	49.4	49.3	49.3	49.5	49.1	49.1	49.0	49.8	50.5	49.9	49.8	50.9	45.1	44.3	44.4	44.1	45.3	24.1
Schmallenberg virus	68.8	70.9		70.0	57.6	56.8	54.5	49.4	49.5	48.1	48.8	47.9	48.5	48.5	48.0	48.1	48.0	49.8	50.1	50.2	49.3	49.3	44.7	44.6	44.7	44.7	45.6	24.6
Simbu orthobunyavirus	71.1	70.1	70.0		58.3	57.6	55.0	49.7	49.2	48.4	48.4	48.3	48.7	48.4	47.1	48.9	47.6	48.8	49.3	48.9	48.4	49.5	44.6	44.5	44.6	44.5	45.5	24.5
Oropouche virus	58.7	58.4	57.6	58.3		66.2	58.8	52.6	52.7	50.2	49.9	49.9	49.8	49.9	49.1	49.0	48.7	51.4	51.5	51.1	49.8	50.4	46.5	45.8	45.7	45.9	46.1	25.0
Oya virus	57.9	57.5	56.8	57.6	66.2		58.0	52.8	52.4	48.6	48.5	48.6	48.2	49.3	48.3	48.9	48.8	50.5	50.6	50.5	49.5	50.1	46.4	45.9	45.9	45.9	45.2	23.6
Leanyer virus	55.3	54.3	54.5	55.0	58.8	58.0		50.7	50.8	49.0	48.4	48.1	48.2	49.2	48.2	49.2	48.8	50.4	50.6	50.3	49.3	48.4	46.2	45.0	45.1	44.8	46.8	24.1
Caraparu virus	49.6	50.6	49.4	49.7	52.6	52.8	50.7		94.4	50.6	51.4	50.5	51.2	51.0	50.2	51.1	50.4	50.7	50.9	50.8	49.2	50.6	46.2	46.5	46.5	46.4	47.3	25.0
Madrid virus	49.7	50.6	49.5	49.2	52.7	52.4	50.8	94.4		50.3	51.4	50.7	51.2	51.2	50.4	51.3	50.6	50.7	51.2	50.8	49.1	50.6	46.3	46.6	46.6	46.5	46.9	25.0
Batai virus	48.3	48.8	48.1	48.4	50.2	48.6	49.0	50.6	50.3		82.8	81.9	80.6	67.2	65.5	66.7	66.6	54.4	55.0	54.0	52.1	51.6	47.6	48.3	48.4	48.0	48.8	25.3
Bunyamwera virus	48.8	49.4	48.8	48.4	49.9	48.5	48.4	51.4	51.4	82.8		91.6	82.1	67.9	65.8	67.4	67.0	55.4	55.9	55.0	52.7	52.0	47.1	47.7	47.6	47.4	48.4	24.9
Ilesha virus	47.7	49.3	47.9	48.3	49.9	48.6	48.1	50.5	50.7	81.9	91.6		81.1	67.6	65.3	67.2	66.9	54.4	55.0	54.3	52.5	52.0	47.2	47.4	47.3	47.1	48.5	24.5
Cache Valley virus	48.6	49.3	48.5	48.7	49.8	48.2	48.2	51.2	51.2	80.6	82.1	81.1		67.7	66.1	66.3	67.2	54.5	55.4	54.6	52.4	51.8	47.8	47.9	47.9	47.5	48.5	25.1
Iaco virus	49.0	49.5	48.5	48.4	49.9	49.3	49.2	51.0	51.2	67.2	67.9	67.6	67.7		86.1	80.2	80.0	54.1	54.3	54.0	51.2	51.9	48.6	47.9	48.0	47.8	48.7	24.9
Sororoca virus	48.1	49.1	48.0	47.1	49.1	48.3	48.2	50.2	50.4	65.5	65.8	65.3	66.1	86.1		78.3	77.6	53.6	53.6	53.2	50.9	52.0	48.6	47.5	47.6	47.6	47.9	24.0
Macaua virus	48.5	49.1	48.1	48.9	49.0	48.9	49.2	51.1	51.3	66.7	67.4	67.2	66.3	80.2	78.3		84.9	55.1	55.4	54.5	50.9	52.0	49.4	48.2	48.3	48.2	48.8	24.6
Wyeomyia orthobunyavirus	47.8	49.0	48.0	47.6	48.7	48.8	48.8	50.4	50.6	66.6	67.0	66.9	67.2	80.0	77.6	84.9		54.7	55.1	54.5	51.0	51.6	49.2	48.2	48.2	48.0	48.1	24.8
Chatanga virus	49.4	49.8	49.8	48.8	51.4	50.5	50.4	50.7	50.7	54.4	55.4	54.4	54.5	54.1	53.6	55.1	54.7		93.7	89.7	57.1	56.4	51.4	52.3	52.2	52.1	49.6	25.0
La Crosse virus	49.2	50.5	50.1	49.3	51.5	50.6	50.6	50.9	51.2	55.0	55.9	55.0	55.4	54.3	53.6	55.4	55.1	93.7		89.5	57.8	57.0	51.6	52.0	51.9	51.8	49.7	25.0
Tahyna virus	49.4	49.9	50.2	48.9	51.1	50.5	50.3	50.8	50.8	54.0	55.0	54.3	54.6	54.0	53.2	54.5	54.5	89.7	89.5		57.9	56.6	51.8	51.4	51.4	51.5	49.9	24.7
Kowanyama virus	47.8	49.8	49.3	48.4	49.8	49.5	49.3	49.2	49.1	52.1	52.7	52.5	52.4	51.2	50.9	50.9	51.0	57.1	57.8	57.9		65.9	47.8	47.4	47.4	47.6	48.1	25.0
Yacaaba virus	49.4	50.9	49.3	49.5	50.4	50.1	48.4	50.6	50.6	51.6	52.0	52.0	51.8	51.9	52.0	52.0	51.6	56.4	57.0	56.6	65.9		49.2	48.8	48.9	48.9	46.9	25.6
Koongol virus	45.3	45.1	44.7	44.6	46.5	46.4	46.2	46.2	46.3	47.6	47.1	47.2	47.8	48.6	48.6	49.4	49.2	51.4	51.6	51.8	47.8	49.2		71.0	70.5	70.8	44.8	24.7
Umbre orthobunyavirus strain Marna (Case #2)	44.1	44.3	44.6	44.5	45.8	45.9	45.0	46.5	46.6	48.3	47.7	47.4	47.9	47.9	47.5	48.2	48.2	52.3	52.0	51.4	47.4	48.8	71.0		98.8	97.9	45.3	24.4
Umbre orthobunyavirus strain Moissiacense (Case #1)	44.2	44.4	44.7	44.6	45.7	45.9	45.1	46.5	46.6	48.4	47.6	47.3	47.9	48.0	47.6	48.3	48.2	52.2	51.9	51.4	47.4	48.9	70.5	98.8		97.6	45.2	24.5
Umbre virus strain IG1424	44.0	44.1	44.7	44.5	45.9	45.9	44.8	46.4	46.5	48.0	47.4	47.1	47.5	47.8	47.6	48.2	48.0	52.1	51.8	51.5	47.6	48.9	70.8	97.9	97.6		45.2	24.3
Murrumbidgee virus	45.5	45.3	45.6	45.5	46.1	45.2	46.8	47.3	46.9	48.8	48.4	48.5	48.5	48.7	47.9	48.8	48.1	49.6	49.7	49.9	48.1	46.9	44.8	45.3	45.2	45.2		24.0
Herbert virus	24.5	24.1	24.6	24.5	25.0	23.6	24.1	25.0	25.0	25.3	24.9	24.5	25.1	24.9	24.0	24.6	24.8	25.0	25.0	24.7	25.0	25.6	24.7	24.4	24.5	24.3	24.0	

Supplementary Table 4: Amino acids identity matrix of the PCR-targeted region on the L-segment (alignment size: 96 AA). See accession numbers in "Phylogenetic analysis".

	Aino virus	Akabane virus	Schmallenberg virus	Simbu orthobunyavirus	Oropouche virus	Oya virus	Leanyer virus	Batai virus	Bunyamwera virus	Ilesha virus	Cache Valley virus	Iaco virus	Sororoca virus	Macaua virus	Wyeomyia orthobunyavirus	Chatanga virus	La Crosse virus	Tahyna virus	Culex pipiens France (C2)	Culex pipiens France (F2)	Culex pipiens France (G2)	Culex pipiens France (C9)	Koongol virus	Little Sussex virus	Umbre virus strain IG1424	Umbre orthobunyavirus strain Marna (Case #2)	Umbre orthobunyavirus strain Moissiacense (Case #1)	Kowanyama virus	Yacaaba virus	Caraparu virus	Madrid virus	Murrumbidgee virus	Salt ash virus	Herbert virus
Aino virus		75.8	81.1	76.8	69.5	64.2	66.3	67.4	68.4	66.3	62.1	62.1	62.1	58.9	61.1	65.3	65.3	65.3	52.6	52.6	52.6	51.6	54.7	61.1	61.1	61.1	61.1	67.4	69.5	61.1	62.1	51.6	58.9	45.8
Akabane virus	75.8		81.1	73.7	67.4	66.3	62.1	63.2	63.2	63.2	61.1	58.9	58.9	55.8	61.1	60.0	64.2	62.1	57.9	57.9	57.9	56.8	62.1	61.1	61.1	61.1	61.1	64.2	68.4	62.1	62.1	50.5	54.7	47.9
Schmallenberg virus	81.1	81.1		78.9	71.6	68.4	73.7	64.2	66.3	63.2	63.2	60.0	61.1	58.9	62.1	68.4	68.4	68.4	57.9	57.9	57.9	56.8	58.9	64.2	64.2	64.2	64.2	72.6	74.7	67.4	67.4	53.7	53.7	51.0
Simbu orthobunyavirus	76.8	73.7	78.9		70.5	68.4	66.3	64.2	66.3	66.3	62.1	57.9	55.8	61.1	58.9	65.3	64.2	64.2	55.8	55.8	55.8	55.8	52.6	62.1	62.1	62.1	62.1	67.4	72.6	62.1	64.2	53.7	55.8	47.9
Oropouche virus	69.5	67.4	71.6	70.5		71.6	68.4	61.1	61.1	62.1	62.1	57.9	57.9	58.9	56.8	66.3	68.4	68.4	57.9	57.9	57.9	56.8	57.9	57.9	57.9	57.9	57.9	71.6	70.5	61.1	62.1	47.4	51.6	44.8
Oya virus	64.2	66.3	68.4	68.4	71.6		65.3	64.2	57.9	60.0	58.9	57.9	57.9	54.7	61.1	61.1	60.0	61.1	55.8	55.8	55.8	54.7	57.9	57.9	57.9	57.9	57.9	61.1	64.2	63.2	62.1	49.5	52.6	43.8
Leanyer virus	66.3	62.1	73.7	66.3	68.4	65.3		63.2	63.2	64.2	63.2	63.2	61.1	65.3	66.3	67.4	67.4	66.3	50.5	50.5	50.5	50.5	52.6	52.6	52.6	52.6	52.6	67.4	64.2	66.3	66.3	50.5	50.5	41.7
Batai virus	67.4	63.2	64.2	64.2	61.1	64.2	63.2		80.0	83.2	82.1	71.6	69.5	64.2	68.4	70.5	68.4	69.5	57.9	57.9	57.9	56.8	63.2	62.1	62.1	62.1	62.1	66.3	61.1	61.1	60.0	56.8	53.7	44.8
Bunyamwera virus	68.4	63.2	66.3	66.3	61.1	57.9	63.2	80.0		92.6	82.1	68.4	68.4	72.6	70.5	70.5	71.6	71.6	51.6	51.6	51.6	51.6	54.7	57.9	57.9	57.9	57.9	66.3	63.2	60.0	61.1	51.6	54.7	44.8
Ilesha virus	66.3	63.2	63.2	66.3	62.1	60.0	64.2	83.2	92.6		85.3	67.4	67.4	71.6	68.4	69.5	71.6	70.5	53.7	53.7	53.7	53.7	56.8	58.9	58.9	58.9	58.9	64.2	61.1	61.1	62.1	52.6	54.7	46.9
Cache Valley virus	62.1	61.1	63.2	62.1	62.1	58.9	63.2	82.1	82.1	85.3		66.3	66.3	66.3	70.5	71.6	70.5	72.6	52.6	52.6	52.6	52.6	56.8	55.8	55.8	55.8	55.8	65.3	61.1	62.1	61.1	50.5	52.6	42.7
Iaco virus	62.1	58.9	60.0	57.9	57.9	57.9	63.2	71.6	68.4	67.4	66.3		89.5	84.2	82.1	62.1	62.1	64.2	57.9	57.9	57.9	56.8	58.9	56.8	56.8	56.8	56.8	61.1	62.1	56.8	55.8	52.6	55.8	40.6
Sororoca virus	62.1	58.9	61.1	55.8	57.9	57.9	61.1	69.5	68.4	67.4	66.3	89.5		80.0	80.0	64.2	64.2	66.3	54.7	54.7	54.7	53.7	62.1	55.8	55.8	55.8	55.8	62.1	63.2	55.8	54.7	51.6	56.8	40.6
Macaua virus	58.9	55.8	58.9	61.1	58.9	54.7	65.3	64.2	72.6	71.6	66.3	84.2	80.0		85.3	63.2	64.2	65.3	52.6	52.6	52.6	52.6	53.7	55.8	55.8	55.8	55.8	62.1	65.3	61.1	62.1	51.6	52.6	39.6
Wyeomyia orthobunyavirus	61.1	61.1	62.1	58.9	56.8	61.1	66.3	68.4	70.5	68.4	70.5	82.1	80.0	85.3		67.4	66.3	69.5	55.8	55.8	55.8	54.7	56.8	60.0	60.0	60.0	60.0	62.1	65.3	62.1	61.1	48.4	50.5	39.6
Chatanga virus	65.3	60.0	68.4	65.3	66.3	61.1	67.4	70.5	70.5	69.5	71.6	62.1	64.2	63.2	67.4		92.6	93.7	57.9	57.9	57.9	56.8	58.9	60.0	60.0	60.0	60.0	73.7	67.4	63.2	62.1	52.6	54.7	44.8
La Crosse virus	65.3	64.2	68.4	64.2	68.4	60.0	67.4	68.4	71.6	71.6	70.5	62.1	64.2	64.2	66.3	92.6		92.6	58.9	58.9	58.9	57.9	61.1	60.0	60.0	60.0	60.0	74.7	69.5	63.2	64.2	53.7	56.8	44.8
Tahyna virus	65.3	62.1	68.4	64.2	68.4	61.1	66.3	69.5	71.6	70.5	72.6	64.2	66.3	65.3	69.5	93.7	92.6		58.9	58.9	58.9	57.9	58.9	60.0	60.0	60.0	60.0	74.7	70.5	64.2	63.2	53.7	56.8	45.8
Culex pipiens France (C2)	52.6	57.9	57.9	55.8	57.9	55.8	50.5	57.9	51.6	53.7	52.6	57.9	54.7	52.6	55.8	57.9	58.9	58.9		100.0	100.0	98.9	83.2	76.8	76.8	76.8	76.8	60.0	57.9	51.6	52.6	54.7	53.7	43.8
Culex pipiens France (F2)	52.6	57.9	57.9	55.8	57.9	55.8	50.5	57.9	51.6	53.7	52.6	57.9	54.7	52.6	55.8	57.9	58.9	58.9	100.0		100.0	98.9	83.2	76.8	76.8	76.8	76.8	60.0	57.9	51.6	52.6	54.7	53.7	43.8
Culex pipiens France (G2)	52.6	57.9	57.9	55.8	57.9	55.8	50.5	57.9	51.6	53.7	52.6	57.9	54.7	52.6	55.8	57.9	58.9	58.9	100.0	100.0		98.9	83.2	76.8	76.8	76.8	76.8	60.0	57.9	51.6	52.6	54.7	53.7	43.8
Culex pipiens France (C9)	51.6	56.8	56.8	55.8	56.8	54.7	50.5	56.8	51.6	53.7	52.6	56.8	53.7	52.6	54.7	56.8	57.9	57.9	98.9	98.9	98.9		82.1	75.8	75.8	75.8	75.8	58.9	56.8	51.6	52.6	54.7	52.6	43.8
Koongol virus	54.7	62.1	58.9	52.6	57.9	57.9	52.6	63.2	54.7	56.8	56.8	58.9	62.1	53.7	56.8	58.9	61.1	58.9	83.2	83.2	83.2	82.1		77.9	77.9	77.9	77.9	61.1	57.9	53.7	54.7	53.7	56.8	40.6
Little Sussex virus	61.1	61.1	64.2	62.1	57.9	57.9	52.6	62.1	57.9	58.9	55.8	56.8	55.8	55.8	60.0	60.0	60.0	60.0	76.8	76.8	76.8	75.8	77.9		100.0	100.0	100.0	60.0	56.8	55.8	56.8	54.7	54.7	40.6
Umbre virus strain IG1424	61.1	61.1	64.2	62.1	57.9	57.9	52.6	62.1	57.9	58.9	55.8	56.8	55.8	55.8	60.0	60.0	60.0	60.0	76.8	76.8	76.8	75.8	77.9	100.0		100.0	100.0	60.0	56.8	55.8	56.8	54.7	54.7	40.6
Umbre orthobunyavirus strain Marna (Case #2)	61.1	61.1	64.2	62.1	57.9	57.9	52.6	62.1	57.9	58.9	55.8	56.8	55.8	55.8	60.0	60.0	60.0	60.0	76.8	76.8	76.8	75.8	77.9	100.0	100.0		100.0	60.0	56.8	55.8	56.8	54.7	54.7	40.6
Umbre orthobunyavirus strain Moissiacense (Case #1)	61.1	61.1	64.2	62.1	57.9	57.9	52.6	62.1	57.9	58.9	55.8	56.8	55.8	55.8	60.0	60.0	60.0	60.0	76.8	76.8	76.8	75.8	77.9	100.0	100.0	100.0		60.0	56.8	55.8	56.8	54.7	54.7	40.6
Kowanyama virus	67.4	64.2	72.6	67.4	71.6	61.1	67.4	66.3	66.3	64.2	65.3	61.1	62.1	62.1	62.1	73.7	74.7	74.7	60.0	60.0	60.0	58.9	61.1	60.0	60.0	60.0	60.0		72.6	65.3	66.3	52.6	55.8	47.9
Yacaaba virus	69.5	68.4	74.7	72.6	70.5	64.2	64.2	61.1	63.2	61.1	61.1	62.1	63.2	65.3	65.3	67.4	69.5	70.5	57.9	57.9	57.9	56.8	57.9	56.8	56.8	56.8	56.8	72.6		62.1	62.1	55.8	54.7	46.9
Caraparu virus	61.1	62.1	67.4	62.1	61.1	63.2	66.3	61.1	60.0	61.1	62.1	56.8	55.8	61.1	62.1	63.2	63.2	64.2	51.6	51.6	51.6	51.6	53.7	55.8	55.8	55.8	55.8	65.3	62.1		97.9	50.5	53.7	43.8
Madrid virus	62.1	62.1	67.4	64.2	62.1	62.1	66.3	60.0	61.1	62.1	61.1	55.8	54.7	62.1	61.1	62.1	64.2	63.2	52.6	52.6	52.6	52.6	54.7	56.8	56.8	56.8	56.8	66.3	62.1	97.9		50.5	53.7	43.8
Murrumbidgee virus	51.6	50.5	53.7	53.7	47.4	49.5	50.5	56.8	51.6	52.6	50.5	52.6	51.6	51.6	48.4	52.6	53.7	53.7	54.7	54.7	54.7	54.7	53.7	54.7	54.7	54.7	54.7	52.6	55.8	50.5	50.5		61.3	37.5
Salt ash virus	58.9	54.7	53.7	55.8	51.6	52.6	50.5	53.7	54.7	54.7	52.6	55.8	56.8	52.6	50.5	54.7	56.8	56.8	53.7	53.7	53.7	52.6	56.8	54.7	54.7	54.7	54.7	55.8	54.7	53.7	53.7	61.3		43.8
Herbert virus	45.8	47.9	51.0	47.9	44.8	43.8	41.7	44.8	44.8	46.9	42.7	40.6	40.6	39.6	39.6	44.8	44.8	45.8	43.8	43.8	43.8	43.8	40.6	40.6	40.6	40.6	40.6	47.9	46.9	43.8	43.8	37.5	43.8	

REFERENCES

1. Peckeu L, Delasnerie-Lauprètre N, Brandel J-P, et al. Accuracy of diagnosis criteria in patients with suspected diagnosis of sporadic Creutzfeldt-Jakob disease and detection of 14-3-3 protein, France, 1992 to 2009. Euro Surveill Bull Eur Sur Mal Transm Eur Commun Dis Bull **2017**; 22.

2. Lasmézas CI, Deslys JP, Robain O, et al. Transmission of the BSE agent to mice in the absence of detectable abnormal prion protein. Science **1997**; 275:402–405.

3. Criscuolo A, Brisse S. AlienTrimmer: a tool to quickly and accurately trim off multiple short contaminant sequences from high-throughput sequencing reads. Genomics **2013**; 102:500–506.

4. Li D, Liu C-M, Luo R, Sadakane K, Lam T-W. MEGAHIT: an ultra-fast single-node solution for large and complex metagenomics assembly via succinct de Bruijn graph. Bioinforma Oxf Engl **2015**; 31:1674–1676.

5. Bigot T, Temmam S, Pérot P, Eloit M. RVDB-prot, a reference viral protein database and its HMM profiles. F1000Research **2019**; 8:530.

6. Buchfink B, Xie C, Huson DH. Fast and sensitive protein alignment using DIAMOND. Nat Methods **2015**; 12:59–60.

7. Wood DE, Salzberg SL. Kraken: ultrafast metagenomic sequence classification using exact alignments. Genome Biol **2014**; 15:R46.

8. Kim D, Song L, Breitwieser FP, Salzberg SL. Centrifuge: rapid and sensitive classification of metagenomic sequences. Genome Res **2016**; Available at: http://genome.cshlp.org/content/early/2016/11/16/gr.210641.116. Accessed 30 November 2018.

9. Truong DT, Franzosa EA, Tickle TL, et al. MetaPhlAn2 for enhanced metagenomic taxonomic profiling. Nat Methods **2015**; 12:902–903.

10. Katoh K, Misawa K, Kuma K, Miyata T. MAFFT: a novel method for rapid multiple sequence alignment based on fast Fourier transform. Nucleic Acids Res **2002**; 30:3059–3066.

11. Katoh K, Standley DM. MAFFT multiple sequence alignment software version 7: improvements in performance and usability. Mol Biol Evol **2013**; 30:772–780.

12. Kearse M, Moir R, Wilson A, et al. Geneious Basic: an integrated and extendable desktop software platform for the organization and analysis of sequence data. Bioinforma Oxf Engl **2012**; 28:1647–1649.

13. Kumar S, Stecher G, Tamura K. MEGA7: Molecular Evolutionary Genetics Analysis Version 7.0 for Bigger Datasets. Mol Biol Evol **2016**; 33:1870–1874.

14. Iwaki T, Figuera M, Ploplis VA, Castellino FJ. Rapid selection of Drosophila S2 cells with the puromycin resistance gene. BioTechniques **2003**; 35:482–484, 486.

15. Ducomble T, Wilking H, Stark K, et al. Lack of evidence for Schmallenberg virus infection in highly exposed persons, Germany, 2012. Emerg Infect Dis **2012**; 18:1333–1335.

16. Reusken C, van den Wijngaard C, van Beek P, et al. Lack of evidence for zoonotic transmission of Schmallenberg virus. Emerg Infect Dis **2012**; 18:1746–1754.

17. Eiden M, Gil P, Ziegler U, et al. Emergence of two Usutu virus lineages in Culex pipiens mosquitoes in the Camargue, France, 2015. Infect Genet Evol J Mol Epidemiol Evol Genet Infect Dis **2018**; 61:151–154.

18. Langmead B, Salzberg SL. Fast gapped-read alignment with Bowtie 2. Nat Methods **2012**; 9:357–359.